Genomic organization of the autonomous regulatory domain of *eyeless* locus in *Drosophila melanogaster*

Shreekant Verma, Rashmi U Pathak and Rakesh K Mishra*

Centre for Cellular and Molecular Biology, Council of Scientific and Industrial Research, Uppal Road, Hyderabad 500007, India

* Corresponding author: email: mishra@ccmb.res.in

Running title: Regulatory domain of *eyeless* locus in *Drosophila*

Key words: Eyeless, chromatin domain boundary, Polycomb response elements, Matrix associated regions, long-range interaction, chromatin domain, gene regulation, *Drosophila*

Abstract

In *Drosophila*, expression of *eyeless* (*ey*) gene is restricted to the developing eyes and central nervous system. However, the flanking genes, *myoglianin* (*myo*), and bent (*bt*) have different temporal and spatial expression patterns as compared to the *ey*. How distinct regulation of *ey* is maintained is mostly unknown. Earlier, we have identified a boundary element intervening *myo* and *ey* genes (ME boundary) that prevents the crosstalk between the *cis*-regulatory elements of *myo* and *ey* genes. In the present study, we further searched for the *cis*-elements that define the domain of *ey* and maintain its expression pattern. We identify another boundary element between *ey* and *bt*, the EB boundary. The EB boundary separates the regulatory landscapes of *ey* and *bt* genes. The two boundaries, ME and EB, show a long-range interaction as well as interact with the nuclear architecture. This suggests functional autonomy of the *ey* locus and its insulation from differentially regulated flanking regions. We also identify a new Polycomb Response Element, the *ey*-PRE, within the *ey* domain. The expression state of the *ey* gene, once established during early development is likely to be maintained with the help of *ey*-PRE. Our study proposes a general regulatory mechanism by which a gene can be maintained in a functionally independent chromatin domain in gene-rich euchromatin.

Introduction

The *Drosophila eyeless* gene (*ey*), a *Pax*-6 homolog, is an essential regulatory gene required for development of the eye (QUIRING *et al.* 1994). It is one of the many evolutionarily conserved genes that are involved in retinal determination. Molecular genetic studies have shown that *ey* along with other genes, viz., *eyes absent* (*eya*), *twin of eyeless* (*toy*), *sine oculis* (*so*), and *dachshund* (*dac*), is involved in retinal determination network (DESPLAN 1997; HALDER *et al.* 1998; PICHAUD AND DESPLAN 2001). Although the genetic interactions of *ey* with these genes are mostly known, spatial and temporal transcriptional regulation of the *ey* is less well understood.

The *ey* gene, present on the fourth chromosome of *Drosophila*, is flanked closely by *myoglianin* (*myo*) gene at the upstream, and *bent* (*bt*) gene downstream. The three genes show a very distinct spatiotemporal pattern of expression in the fly. The expression of *ey* is restricted to eye disc primordia and central nervous system (CNS) during embryogenesis. Later during larval stages it is expressed in eye imaginal discs and CNS, where it continues to express in adults (QUIRING *et al.* 1994; HAUCK *et al.* 1999; ADACHI *et al.* 2003; CHINTAPALLI *et al.* 2007). Unlike *ey, myo* gene that codes for a TGF-β superfamily protein has a high-level of maternal transcript deposition in the early embryo. Later, it expresses in the somatic, visceral, and heart musculature where its expression persists throughout embryogenesis. In third instar larvae, *myo* expression is restricted to brain and glial cells of the ventral nerve cord (LO AND FRASCH 1999; CHINTAPALLI *et al.* 2007). Likewise, the *bt* gene encodes for a titin superfamily muscle protein 'Projectin'. During development, the *bt* transcripts first appear in the mid-embryo stage and increase steadily till the adult stage (FYRBERG *et al.* 1992; MAROTO *et al.* 1992). The expression of *bt* has been found in the embryonic/larval muscles system and all types of muscles in pupae and adults (AYME-SOUTHGATE *et al.* 1991; FRISE *et al.* 2010).

Transcriptional regulation of *ey* at various developmental stages by multiple *ey* enhancers has been reported in two earlier studies (HAUCK *et al.* 1999; ADACHI *et al.* 2003). An initial study has identified a 212-bp eye-specific enhancer at 3' end of the second intron that is essential for expression of *ey* in larval eye-disc primordia (HAUCK *et al.* 1999). A later study has described a 5 kb upstream region and a 3.6 kb

second intronic fragment that act synergistically to specify the *ey* specific expression pattern of lacZ reporter construct in developing CNS (ADACHI *et al.* 2003). The targeted expression of *ey* induces ectopic eyes in *Drosophila* (HALDER *et al.* 1998). This suggests that active repression of *ey* is crucial in other tissues, wherever it is not required. However, what maintains the repressed status of *ey* in such tissues, is not known. The distinct spatiotemporal expression of *ey* calls for the presence of other *cis*-regulatory elements like chromatin domain boundary elements (CBEs) or insulators, and also a memory element like Polycomb response elements (PREs). Such *cis*-elements at *ey* locus are required to prevent the cross-talk among the regulatory elements of the three genes and for maintenance of tissue-specific expression, as is the case at several well characterised loci like bithorax complex in *Drosophila* (MAEDA AND KARCH 2006; MIHALY *et al.* 2006).

Boundary elements are an established regulatory feature of most eukaryotic genomes. They insulate a gene from the influence of neighbouring chromatin and actively subdivide the genome into chromatin domains of independent gene activity. The regulatory function of these elements is dependent on their association with several boundary interacting proteins including BEAF-32, CTCF, Su(Hw), Zw5, GAGA factor (GAF or Trl) and CP190 (GEYER *et al.* 1986; KELLUM AND SCHEDL 1991; GERASIMOVA AND CORCES 2001; WEST *et al.* 2002; GASZNER AND FELSENFELD 2006; VALENZUELA AND KAMAKAKA 2006). On the other hand, PREs also known as Cellular Memory Modules (CMMs) are specific DNA elements, recruitment sites for Polycomb group and trithorax group (PcG/trxG) of proteins, that are required to maintain the transcriptional states of the target genes(SIGRIST AND PIRROTTA 1997; CAVALLI AND PARO 1998). The PcG proteins are required for stable silencing, whereas trxG proteins promote activation of target genes. Many PREs studied in *Drosophila* suggest their role in maintenance of repressed states. One such example is *iab7*-PRE in the *Drosophila* bithorax complex, The *iab7*-PRE helps in appropriate maintenance of *Abd-B* gene expression pattern in parasegement 12 (MISHRA *et al.* 2001). Studies based on techniques such as FISH and chromosome conformation capture (3C) assay, support interactions among CBEs and other regulatory elements like promoters, enhancers and silencers. This leads to the formation of chromatin domains with autonomous regulatory function (DEKKER *et al.* 2002; BANTIGNIES *et al.* 2003; RONSHAUGEN AND LEVINE 2004; LANZUOLO *et al.* 2007; SEXTON *et al.* 2009; HOU

et al. 2012; ZHANG *et al.* 2013). These higher order organization of chromatin interaction are known as topological associated domains (TADs). (HOU *et al.* 2012; SEXTON *et al.* 2012; ZHANG *et al.* 2013; CUBENAS-POTTS *et al.* 2017). Anchoring of regulatory elements to nuclear architecture also helps in compartmentalization of the locus into functionally independent domain (PATHAK *et al.* 2007).

In the present study, we have analyzed the *ey* locus to identify *cis*-regulatory elements that define its precise and distinct expression pattern. Earlier, we have identified a CBE upstream of *ey* that separates regulatory domains of *myo* and *ey* genes (SULTANA *et al.* 2011). Here, we have identified a CBE between *ey* and *bt*, two closely spaced but distinctly expressed genes. We refer to this element as EB boundary and functionally characterize it in the transgenic context. Additionally, we have identified a PRE (*ey*-PRE) that functions as a repressor to maintain the expression pattern of *ey*. Furthermore, to understand the mechanism of *ey* regulation by EB, *ey*-PRE, and previously identified ME boundary, we have explored their long-range interactions in the context of nuclear architecture. Our findings reveal two new regulatory elements in this important locus, and the structural framework of this genomic locus based on the higher-order chromatin organization of regulatory elements. Such organization may have a general implication in higher eukaryotes.

Results

Identification of potential CBEs that separate ey and bt loci

Previously, we have identified a CBE (the ME boundary) in the ~1.6 kb intergenic region between *myo* and *ey* genes, endorsing the rationale that CBEs are required to prevent crosstalk between the regulatory elements of closely spaced but differently expressed genes (SULTANA *et al.* 2011). Likewise, *ey* and the downstream gene *bt,* have a disparate pattern of expression (AYME-SOUTHGATE *et al.* 1991). Therefore, we expected a CBE to be present in the 3.2 kb intergenic region to block crosstalk between the adjacent regulatory domains. To identify a potential CBE between *ey* and *bt*, we used cdBEST search tool which has been successfully utilized to identify several new CBEs in *Drosophila* and other insects like *Anopheles*

gambie (SRINIVASAN AND MISHRA 2012; AHANGER *et al.* 2013). CdBEST predicts CBEs based on the presence of clusters of binding motifs of many known boundary proteins like BEAF-32, CTCF, GAF, CP190, and *Zw5,* in the queried sequence.

CdBEST analysis for the ~30 kb *ey* locus predicted two CBEs, one being the previously reported ME boundary and a new putative CBE in the seventh intron of *ey* gene (INT7) (Figure 1). No CBE is predicted in the intergenic region between *ey* and *bt,* although the region carried multiple binding motifs of BEAF-32, CTCF, and GAF. Therefore, we analyzed the data available for *in-vivo* binding of boundary proteins in this region using embryonic genome-wide ChIP-chip datasets from the modENCODE project (http://www.modencode.org/) (NEGRE *et al.* 2010). We observed a significantly high occupancy of CTCF and CP190 in a ~1.2 Kb region within INT7. However, a prominent binding of both of these proteins is also observed in the ~2.2 Kb region between *ey* and *bt* (EB). Particularly, CTCF binding at EB occurs in two separate regions, one in a ~0.8 kb 3' UTR region of *ey* (named as EB-u), and the other in adjacent ~1.1 kb intergenic region (named as EB-i). EB-i additionally has binding of BEAF-32. We did not find a significant binding of GAF in these regions (Figure 1).

As the existence of DNaseI hypersensitive sites (DHS) are inherent feature of regulatory elements, including several known CBEs we next examined the presence of DHS in INT7 and EB using the DHS dataset of embryonic stage 9 (6 h embryo) available at UCSC genome browser (http://genome.ucsc.edu/) (THOMAS *et al.* 2011). Both INT7 and EB contained a prominent DHS (Figure 1 and b). These observations altogether indicate potential CBE function of INT7 and EB (Figure 1b, Supplementary Figure 1, Supplementary Table 1).

EB functions as an enhancer blocker in the eye

To test the boundary activity of INT7 and EB, we generated transgenic flies carrying test fragments introduced between the *white* enhancer and *mini-white* reporter gene in enhancer blocker assay construct (pRW+) (Figure 2a) (HAGSTROM *et al.* 1996). The level of eye pigmentation in adult transgenic flies is a responsive indicator of the amount of *mini-white* transcription. In case a CBE placed between the enhancer

and *mini-white* acts as an enhancer blocker, it would reduce the level of *mini-white* expression that can be scored as light eye colour in adult flies. However, a random DNA fragment in the same position would have no effect (HAGSTROM *et al.* 1996). The test fragments in the assay vector are flanked by *lox*P sites so that it can be flipped out using the *cre-lox*P system to confirm the enhancer blocker effect and rule out any position effect.

All the transgenic fly lines generated for INT7 had a high level of eye pigmentation (red to bright red eye colour) in heterozygous condition. Moreover, the removal of INT7 in four such initial lines (P) did not change in the level of eye pigment in their flipped-outs (ΔP) indicating that INT7 lacked an enhancer-blocker activity (Figure 2b, Supplementary Table 2). In contrast, seven transgenic lines carrying EB fragment displayed varying degrees of light red eye colour in heterozygous conditions, and four of them turned darker when EB was flipped out. We found a mild increase in eye colour in all EB flipped-out lines, and at least one of them showed a ~2-fold increase in eye pigment level (Figure 2b, Supplementary Table 2). Homozygous (P/P) transgenic lines mostly showed a high level of eye pigmentation (dark red eye colour) for both the INT7 and EB transgenes. These results suggested that the EB acts as a weak enhancer blocker in the eye and the flipped-out lines confirmed that light eye colour is due to the boundary function of EB and not a position effect.

As explained in the earlier section, EB can be split into two fragments based on CTCF binding sites as EB-u and EB-i. The binding of BEAF-32, however, is detected only in the EB-i region. Both of these regions contain distinct DHS, which is more prominent in the EB-i (Figure 1b). We further tested the enhancer blocking activity of both the fragments separately, to identify whether the boundary function lies in one of these regions or the entire EB sequence is required for the activity. All the EB-u transgenic lines had dark red eye colour and did not exhibit enhancer-blocker effect as no change in eye colour was observed in flipped-out lines. In contrast, EB-i transgenic lines showed light eye colour, and five out of seven lines showed a mild (~1.5 fold) increase in eye colour after P-element flipping out, suggesting that enhancer blocker activity of EB mainly resides in EB-i (Figure 2b, Supplementary Table 2).

In summary, the presence of DHS with significant boundary proteins occupancy at INT7 and EB suggested their boundary features, but only EB displayed enhancer blocker effect in the adult eye. As the CBE features were observed using datasets from embryonic developmental stages, we reasoned that these regions might be functional as a boundary mostly during early development. Therefore, we tested the boundary activity of INT7 and EB in the embryo.

EB functions as an enhancer blocker in embryo

We used a P-element based CfhL assay vector to test boundary activity in developing embryos (Figure 3a) (HAGSTROM *et al.* 1996). The construct carries two reporter genes *mini-white* and *hsp70/lacZ.* Two *ftz* enhancers, an upstream enhancer (UPS) active during early development and a late neurogenic enhancer (NE), drive the *hsp70/lacZ* in the embryo. The level of eye pigmentation and x-gal staining in the embryo both indicates the expression level of *mini-white* and *lacZ*, respectively. A test DNA inserted between the *lacZ* promoter and the enhancers that act as an enhancer blocker causes a reduced level of *lacZ* expression. The test element can be flipped out in transgenes to confirm the enhancer-blocker activity and rule out any position effect. In addition, the *mini-white* expression level in the eye can be compared to rule out a repressor effect of the test elements (HAGSTROM *et al.* 1996; SULTANA *et al.* 2011).

In EB transgenic lines, we observed significantly reduced X-gal staining in both early and late embryonic stages suggesting EB prevented both the enhancers from acting on *lacZ* (Figure 3b-c and Supplementary Figure 2). EB in homozygotic condition displayed a strong boundary activity which was similar to the known *Fab7* boundary (HAGSTROM *et al.* 1996). In two out of three EB flipped out version of the transgenic lines, an intense X-gal staining was restored (comparable to empty vector). At the same time, the eye colour remained the same, suggesting that EB functions as an enhancer blocker but not a repressor (Figure 3b-c, Supplementary Figure 2 and Supplementary Table 3). Interestingly, INT7 transgenes also displayed a weak enhancer blocker activity in the embryo. Two out of three transgenic lines of INT7 showed a moderate increase in the X-gal staining in both early and late stages embryos after flipping out the test elements (Figure 3b-c, Supplementary Table 3,

Supplementary Figure 2). When EB-u and EB-i fragments were tested separately, EB-u did not exhibit any enhancer blocker activity in the embryo as an intense X-gal staining comparable to empty vector was observed. The EB-i region, on the other hand, showed a strong enhancer blocker activity, comparable to EB. Like EB, flipped out EB-i lines showed a significant increase in the X-gal staining with no change in eye colour. These observations indicated that mainly the EB-i, which carries BEAF-32 binding sites harbours the boundary activity in this region (Figure 3b-c, Supplementary Figure 2 and Supplementary Table 3). Altogether these results suggest that EB and INT7 are active boundaries during embryonic development. Further, a weak enhancer blocker activity of INT7 in the embryo suggest its assistive function to EB (a strong boundary) in demarcating the *ey* locus.

Identification of a putative PRE associated with ey locus

It is known that multiple enhancers positively regulate the *ey* gene in developing eye and CNS (HAUCK *et al.* 1999; ADACHI *et al.* 2003). However, the regulatory elements that maintain the repressed state of *ey* in other tissues are not known. In *Drosophila,* PREs are involved in establishing and keeping the repressed state of genes (MISHRA *et al.* 2001; AMERICO *et al.* 2002). We, therefore, searched for putative PRE in *ey* locus using a Perl-based PRE mapper tool (SRINIVASAN AND MISHRA 2020). This tool uses a motif cluster search of known DNA binding PcG recruiters like Pho, GAF, Dsp1, Sp1, and Cg. PRE mapper predicted a ~1.6 kb putative PRE region upstream of the exon 1 of *ey.* We named this element as *ey*-PRE, and observed that it has clusters of Sp1 (3), Cg (3), Pho (1), and GAF (1) binding sites in an internal core region of ~800 bp. Interestingly, the *ey*-PRE also contained a second *ey* promoter region that is predicted in the eukaryotic promoter database (DREOS *et al.* 2015) (Figure 4).

To assess whether the *ey*-PRE is a target of PcG proteins, we looked into the presence of repressive histone modification (H3K27me3) and binding of PcG proteins (PRC1 members - Pc, Psc, and dRing) using ChIP-seq data of 14-16h embryo available at the modENCODE database (MOD *et al.* 2010). We observed an H3K27me3 domain with significant enrichment of Pc in *ey* locus. Interestingly, the repressive H3K27me3 modification is primarily confined to *ey* locus only, whereas

flanking regions toward *myo* and *bt* hold active histone modification of H3K27ac. At the same time, boundary proteins namely BEAF-32, CP190, and CTCF (Chip-seq data from modENCODE project) are present at both, ME and EB boundaries that demarcate the borders of the repressive domain of *ey* (Figure 4c). Presence of a Pc-enriched repressive domain restricted to *ey* locus indicates that a repressive *cis*-acting element is very likely to be present within the locus. Additionally, bindings of PcG proteins Pc, dRING, and Psc in a significantly high amount as a sharp peak at putative *ey*-PRE further strengthens the idea. The ~800 bp internal core region also contained a DHS. With such strong indications for the presence of a functional PRE at the *ey* locus, we decided to test both *ey*-PRE and a smaller fragment of core DHS region, *ey*-dPRE, for PRE activity (Figure 4b, Supplementary Table 1).

ey-PRE functions as a PRE

To determine the PRE potential of *ey*-PRE, we assessed the repressor activity of full-length *ey*-PRE (~1.6kb) and *ey*-dPRE (831 bp) in the adult eye using a previously described pCasper vector-based transgene assay (Figure 5a). In this assay, the presence of a PRE upstream of the *mini-white* gene causes its repression resulting in reduced and variegating eye colour (VASANTHI *et al.* 2013). We observed both repression and variegation of *mini-white* in the *ey*-PREs transgenic lines. Of the *ey*-PRE transgenic lines, 52% (16 out of 31) lines showed lighter eye colour, and 55% (18 out of 31) lines showed variegation. In the case of *ey*-dPRE, 50% (13 out of 26) lines displayed lighter eye colour while 21% (4 out of 19) lines showed variegation (Figure 5b, Table 1, and Supplementary Table 4). Further, to confirm that the repressive activity of *ey*-PRE and *ey*-dPRE is not a position effect, we excised out the PREs. Excision of *ey*-PRE/*ey*-dPRE led to the de-repression of *mini-white* in both sets of transgenic lines (Figure 5b and Table 1). Specifically, 59% and 47% of *ey*-PRE and *ey*-dPRE lines, respectively, showed an increase in the eye colour after flipping out of the transgene. Interestingly, we also observed a loss of variegation in the flipped-out lines of both the transgenes confirming the repressor function of *ey*-PRE/*ey*-dPRE.

One of the well-known characteristics of PREs is pairing-sensitive silencing (PSS), where in homozygous conditions, a PRE transgene results in stronger repression as

compared to the heterozygous lines (KASSIS 1994; KASSIS 2002; KASSIS AND BROWN 2013). In our assay, >30% of the *ey*-PRE/*ey*-dPRE lines, showed a strong PSS effect in homozygous condition, which is lost in flipped-out lines (Figure 5b, Table 1, and Supplementary Table 4).

In the next step, to ascertain whether the repressor activity of *ey*-PRE/*ey*-dPRE is PcG protein-dependent, we brought a few representative *ey*-PREs lines into mutations background of different PcG proteins by crossing homozygous *ey*-PRE males to the females carrying PcG mutations (Table 2). We compared the de-repression of *mini-white* scored as an increase in the eye pigment level in the progenies from these crosses carrying *ey*-PRE with and without PcG mutation. We found that mutation in *Psc* gene (Psc^1 allele) caused a notable de-repression of *mini-white* in five of *ey*-dPRE lines tested. Mutation alleles of *Pleiohomeotic* (Pho^1) and *Polycomb* (Pc^1) in heterozygous condition exhibited very mild de-repression of *mini-white*. However, a double PcG mutation of Psc^1 and Pc^1 causes cumulative de-repression effect (Figure 5c, Table 2). We also tested GAF mutation (Trl^{R85}) as we observed its binding at *ey*-PRE region (Figure 4), and interestingly loss of GAF caused a notable de-repression (Figure 5c-d and Table 2). These observations suggest that while the function of *ey*-PRE is dependent on PcG genes as in the case of typical PREs, it is possible that factors other than PcG proteins, like GAF, are also involved in its repressive functions. Our observation is supported by earlier reports where GAF has been shown to interact with a *Drosophila* PRE (MISHRA *et al.* 2001).

ME interacts with EB and ey-PRE

As the two CBEs, ME and EB sharply demarcate *ey* locus, we wanted to investigate whether these regions interact in a long-range to mark independent chromatin domain of *ey* regulation. We performed 3C in the 0-16h embryo. Using all forward primers to PCR amplify the ligated hybrids (3C DNA) we calculated the interaction frequency of ME with several regions at *ey* locus by gel quantification method as described in Naumova et al.(NAUMOVA *et al.* 2012). Additionally, hybrid template controls were generated to assess the forward primer pair efficiency. The fragment comprising ME boundary showed a high interaction frequency with *ey*-PRE and a

lesser but significant interaction frequency with EB and an internal region of *ey* (Figure 6a-b). However, we did not detect any such interaction of ME with immediate upstream *myo* gene, or further downstream *bt* gene.

To understand the *ey* domain organization even better and to validate our 3C results, we explored these interactions in previously published Hi-C data from the whole embryo and a late embryo-derived Kc167 cell, using an online web tool juicebox.js (SEXTON *et al.* 2012; LI *et al.* 2015; CUBENAS-POTTS *et al.* 2017; EAGEN *et al.* 2017; ROBINSON *et al.* 2018). A visual inspection of the fourth chromosome Hi-C heatmap from the embryo (SEXTON *et al.* 2012) revealed that *ey* and *bt* genes exist in a TAD. While *myo*, present in a distinct domain upstream region to *ey*, is separated by ME boundary (Supplementary Figure 3). We next looked into the details of chromatin looping within the *ey* TAD, in high-resolution Hi-C data available for Kc167 cells (CUBENAS-POTTS *et al.* 2017; EAGEN *et al.* 2017). In these Hi-C data, *ey* and *bt* are found to reside in an independent sub-domain within the same TAD. However, *myo* and *MED26* are part of separate domains (Figure 6b and Supplementary Figure 3). The ME boundary appears to be in contact with EB boundary (Figure 6b). We compared the expression profile of these genes in Kc167 cells to further understand the functional relevance of domain organization at *ey* locus (CHERBAS *et al.* 2011). Interestingly, we observed that *ey* and *bt* are expressed at a very low level suggesting their co-regulation in a transcriptionally inactive domain. In contrast, *myo* and *MED26* show a higher level of expression (Supplementary Figure 3). We also used the data available at 4Dgenome (https://4dgenome.research.chop.edu/), which predicts enhancer-promoter interactions, to look into the interactions within *ey* region (HE *et al.* 2014). This data also indicates the interaction of ME to *ey*-PRE and downstream *ey* regions, similar to our observation (Figure 6b). These observations together suggest the interaction of ME boundary with *ey*-PRE. Also, the interaction of ME with EB in the embryo and Kc167 cells reflects the role of the two CBEs in defining a functional chromatin domain.

ME, EB and ey-PRE associate differently with nuclear matrix

Nuclear Matrix (NuMat) has been proposed to provide a structural framework for targeted tethering of chromatin domain in sub-nuclear space (MISHRA AND KARCH

1999). DNA that associates with NuMat (MARs) are proposed to be the anchoring sequence. CBEs have been shown to associate with each other and along with boundary proteins are shown to associate NuMat (BLANTON *et al.* 2003; BYRD AND CORCES 2003; PATHAK *et al.* 2007). As we have observed interaction amongst ME, EB, and *ey*-PRE, we further investigated their NuMat association potential using an *in vivo* MAR assay (MIRKOVITCH *et al.* 1984) (Supplementary Figure 4). In the assay, an equal amount of PCR amplified test regions was Southern hybridized with radio-labelled NuMat DNA isolated from *Drosophila* embryos. NuMat association is determined by comparative quantification of hybridization signal of test regions with known MAR region in Histone gene (HIS-MAR) and a non-MAR region in exonic sequence of the BEAF-32 gene (BEAF-CDS) (MIRKOVITCH *et al.* 1984; PATHAK *et al.* 2007).

We found that ME and EB both show a comparable level of association with NuMat. Interestingly, the *ey*-dPRE and the (EB-u region) 3'-UTR of *ey* gene also show a strong association with NuMat. However, the INT7 region does not show any significant association with NuMat (Figure 7). During embryonic development, *ey* expresses in limited number of cells, i.e., eye-antennal disc primordium, and embryonic brain cells (HAUCK *et al.* 1999). Reasoning that we might be losing important information as *ey* does not express in over-whelming majority of embryonic cells, we also tested the NuMat association of the locus in a different tissue with significant *ey* transcriptional activity, i.e., brain-eye-antennal imaginal discs of third instar larvae. In third instar larvae, *ey* mainly expresses in CNS and anterior to the morphogenetic furrow in the eye disc. As the other extreme, we also tested NuMat association of *ey* locus in S2 cells where the gene is not transcribed (CZERNY *et al.* 1999; HAUCK *et al.* 1999; ADACHI *et al.* 2003; CHINTAPALLI *et al.* 2007). The NuMat associations of ME, *ey*-PRE, and EB varied in the embryo, brain-eye-antennal disc, and S2 cells. Interestingly, *ey*-PRE was found to associate with NuMat in all the tissues examined, irrespective of *ey* gene transcription status. ME and EB boundaries were found to associate with NuMat in embryos and brain-eye disc, while the association was completely absent in S2 cells. EB-u association to NuMat is stronger than EB-i, indicating that while EB-i harbours boundary activity, EB-u is responsible for tethering of the locus to nuclear architecture (Figure 7). The differential association of *ey cis*-regulatory elements to NuMat indicates that *ey* locus

may be organized differently in different cell types depending on the transcriptional activity of the locus. While these observations provide an initial clue to the 3D organization of the locus, detailed studies will be needed to fully understand the role of MAR sequences in dynamics of the region.

Discussion

The *ey* gene in *Drosophila*, a gene crucial for eye development, is differentially expressed in comparison to its neighbouring genes, *myo,* and *bt*. Adjacent genes, *myo,* which is upstream to *ey,* and *bt,* which is downstream, are very close to *ey*, ~1.6 kb, and ~3.2 kb apart, respectively. Genetic studies have mainly revealed the interaction of *ey* to other genes involved in eye development network (DESPLAN 1997; HALDER *et al.* 1998; PICHAUD AND DESPLAN 2001), but transcriptional regulation *of ey* is not fully understood. Earlier, we have identified ME boundary in the *myo* and *ey* intergenic region (SULTANA *et al.* 2011). Based on the distinct expression pattern of the three genes, we had proposed that additional *cis*-regulatory elements like CBEs and PREs might be present at this locus. In order to identify such elements and to understand their potential role in *ey* regulation, we used bioinformatics prediction tools and clusters of binding sites of known CBEs and PREs binding proteins from genome-wide localization studies. We further co-mapped the region to DHSs that are often indicative of the presence of regulatory elements. Taking clues from *in silico* prediction, we have identified and functionally characterized a novel CBE and a PRE associated with *ey* locus. We show that ~1.2 kb intergenic region between *ey* and *bt*, EB, functions as boundary and ~1.6 kb region, upstream to *ey* promoter, *ey*-PRE, functions as PcG dependent repressor.

Our *in silico* analysis estimates three putative CBEs in *ey* locus, i.e., ME, INT7 and EB. Of these, ME boundary has already been characterized earlier. In the present work, we report that only EB displays a resolute boundary activity during embryonic development as well as a mild boundary activity in the adult stages. Whereas, INT7 shows a scant boundary activity only during early embryogenesis suggesting boundary activity of these elements could be developmentally regulated. A few recent studies have suggested a developmental and tissue-specific regulation of CBEs mediated by spatially and temporally controlled expression of boundary

proteins (AOKI *et al.* 2008; LIN *et al.* 2011; AOKI *et al.* 2012; MATZAT *et al.* 2012; BONCHUK *et al.* 2015; WOLLE *et al.* 2015; GAMBETTA AND FURLONG 2018). For example, expression of boundary factors, Elba and a late boundary complex (LBC), mediate boundary functions of Fab7 element in early embryogenesis and adults, respectively (AOKI *et al.* 2008; AOKI *et al.* 2012; WOLLE *et al.* 2015). In another example, a tissue-specific protein Shep has been shown to modulate *gypsy* boundary activity and nuclear localization, particularly in CNS (MATZAT *et al.* 2012). Our study of *ey* locus presents a similar scenario, where the boundaries are spatially and temporally regulated depending on the transcriptional activity of the locus. It would be further interesting to see if ME, EB and INT7 functions are developmentally regulated or restricted to specific cell-types.

Previous studies have shown that interaction of BEAF-32 with CP190 mediates long-range chromosomal contact, and more than 70% of BEAF-32/CP190 bindings demarcate domain boundaries in the *Drosophila* genome (VOGELMANN *et al.* 2014; CUBENAS-POTTS *et al.* 2017; WANG *et al.* 2018). The EB element also harbours *in vivo* binding sites of BEAF-32, CP190, and CTCF co-mapping with a prominent DHS. This overall architecture of the EB element shows a remarkable similarity to the earlier identified ME (SULTANA *et al.* 2011). These evidences suggest that the same molecular players, particularly BEAF-32 and CP190, might be contributing to the functional linking of the two CBEs to define the loop domain of *ey*. In our 3C experiment, we confirm the interaction between ME and EB suggesting that the two CBEs, flanking the *ey* locus, define functional autonomy of the chromatin loop domain. In support to our finding, we observe the chromatin loop of ME with EB in HiC data from previous studies in Kc167 cells which places *ey* in an independent domain within a larger TAD (LI *et al.* 2015; CUBENAS-POTTS *et al.* 2017; EAGEN *et al.* 2017). These interactions provide necessary insulation to *ey* locus from the neighbouring regulatory environments.

We report here the identification and functional validation of a new CMM or PRE, *ey*-PRE, within the *ey* domain. Besides conferring a repressive feature in the transgene-based assay, the element also exhibits PSS. The *ey*-PRE element encompasses a core DHS region spanning ~830 bp (*ey*-dPRE) that coincides with sharp binding peaks of PcG proteins of PRC1 members, Pc, Psc, dRing. However, in the

transgene, we could only see a prominent de-repressive effect of Psc mutation. Other PcG proteins show a moderate and varying impact on *ey*-PRE activity, which could be because these mutations were tested in heterozygous condition, as homozygous mutants are lethal. In case of double PcG mutants however we could see strong de-repression effect which suggests that *ey*-PRE maintains the expression state of the *ey* locus and requires the activity of a subset of PcG proteins for the purpose. This property of *ey*-PRE is similar to the earlier reported PREs (KASSIS 2002; KASSIS AND BROWN 2013). Interestingly, GAF protein was also found to attenuate the function of *ey*-PRE. ME boundary also has been reported to interact with GAF protein (SULTANA *et al.* 2011). The observed 3C interaction of ME and *ey*-PRE could be mediated by GAF protein. Recent HiC studies also support the interaction of PREs with multiple regions within a TAD and active role of GAF proteins in such connections (OGIYAMA *et al.* 2018). The *ey*-PRE also has predicted promoter property, which suggest it to have a dual role of promoter as well as CMM. However, the role of GAF remains unexplored and it will be interesting to see if GAF is crucial to these functions.

Studies have shown that NuMat provides anchoring sites for the compartmentalization of higher-order chromatin organization and also acts as a platform for functional activities inside the nucleus. Work from our lab and elsewhere have shown that boundary elements function in the context of NuMat (BYRD AND CORCES 2003; PATHAK *et al.* 2007). In this study, we show that multiple sites of the *ey* locus, including ME, *ey*-PRE, and EB, associate with NuMat in cell type and transcription status dependent manner. As BEAF-32 is a bona fide NuMat associated protein in flies, and ME and EB, both carry BEAF-32 binding sites, the anchoring of these CBEs to the nuclear architecture is probably mediated by the protein (PATHAK *et al.* 2007). The prominent association of ey-PRE to NuMat in all cell types, unlike other elements, suggests the role of the memory element in all functional states or cell types. Taken together, the dynamic nature of NuMat association of different regulatory elements of the locus supports the hypothesis that depending on the expression state, *ey* locus is present in separate compartments and that NuMat might be providing the structural basis for this compartmentalization.

Based on these findings, we propose a model for *ey* gene expression where *ey*-PRE functions as both PRE/TRE to maintain the active or repress state of *ey* in different cell/tissues initially established by early developmental cues. The CBEs, ME and EB, demarcate the *ey* locus, to create an independent domain of *ey* differential regulation from the neighbouring genes *myo* and *bt,* by chromatin looping and thus prevent the cross talk among the regulatory elements of the adjacent genes. The *ey*-PRE, perhaps with the other unidentified regulatory elements of *ey* locus, which are bound to PcG or TrxG proteins, takes the *ey* domain either to repressive (*Polycomb* body) or active (transcription factory) compartments, respectively (Figure 8).

Conclusions

In conclusion, we have identified boundary elements, ME and EB, that demarcate the *ey* domain and a cellular memory element, *ey*-PRE, within this domain. In order to get insight into the mechanism of *ey* regulation, we have investigated how these regulatory elements function together in their genomic context. We have learnt that long-range interactions of ME with *ey*-PRE and EB, along with their discrete association to the NuMat brings about the tissue-specific regulation of *ey*. As *ey* expresses only in a discrete group of cells, while in the majority of cells in the embryo or a tissue it remains repressed, it is challenging to compare higher-order chromatin organizational changes at the locus during embryonic development. However, one way to unearth such mechanisms is to carry out super-resolution imaging of the locus in a cell-type-specific manner. Further, identification of molecular players involved in the long-range interactions and the NuMat association of these regulatory elements will also provide an insight into the regulation of the locus. At present, this study offers a working model for the underlying mechanism of *ey* spatiotemporal regulation in *Drosophila*. Our study provides clues to the hierarchical genomic conformational features, that form the basis of gene regulation in euchromatin.

Methods

CBEs and PRE prediction in ey locus

A ~ 30 kb *ey* region was used in cdBEST analysis to identify new CBEs at *ey* locus. Additionally, for prediction of the CBEs, *in-vivo* binding of known boundary proteins BEAF32, CP190, CTCF, and GAF was analyzed using whole embryo (0-12 h) ChIP-chip data from a previous by study Negre et al., 2010(NEGRE *et al.* 2010). We co-mapped the DNaseI hypersensitive sites(DHS) in the region using stage-9 (~ 6 h) embryo DHS data available at UCSC browser (https://genome.ucsc.edu/) (THOMAS *et al.* 2011). Two potential CBEs, a ~ 1.3 kb intronic region in a seventh intron (INT7) and a ~ 2.2 kb intergenic region between *ey* and *bt* (EB), were identified that also co-map with DHS (Figure 1).

A Perl based program, PRE mapper, was used to predict putative PRE (*ey*-PRE) in the *ey* locus (SRINIVASAN AND MISHRA 2020). PRE mapper analyzes motifs of known PRE binding proteins (Pho, GAF, Dsp1, Sp1, Zeste, Grh, Adf1, and Cg), their binding patterns, and motif clustering to define a PRE. Presence of DHS at ey-PRE was reviewed to correlate its regulatory feature. Additionally, a comprehensive analysis of various chromatin features in the *ey* region was carried out using 14-16-h whole embryo ChIP-seq data available at modENCODE by Gary Karpen. modENCODE id of the data used are H3K27Ac (4120), H3K27Me3 (3955), Pc (3957), dRING (5071), Psc (3960), BEAF-32 (3954), CP190 (3959), CTCF (5069), and GAF (4149) (MOD *et al.* 2010).

Cloning of predicted CBEs and PRE

All the test fragments were PCR amplified from *CantonS* fly genomic DNA by high fidelity *Pfu* polymerase with specific primers (Supplementary Figure 1, Supplementary Table 1 and 5). All CBE test fragments (INT7, EB, EB-u and EB-i) were inserted first at MCS in pLML and then sub-cloned along with *loxP* at XhoI sites in the enhancer-blocker assay vectors, pRW+ and pCfhL, (SULTANA *et al.* 2011). Test PREs (*ey*-PRE and *ey*-dPRE) were cloned initially at SmaI blunt site in pLML, then sub-cloned along with *loxP* at XhoI in pCasPerX (VASANTHI *et al.* 2013).

Fly culture, transgenic flies, and genetic crosses

All fly strains of *Drosophila melanogaster* were cultured in standard cornmeal

605 medium at 25 ^{0}C. Transgenic flies were generated by micro-injection of an assay
606 vector DNA and a transposase expressing plasmid *pΔ2-3* together into pre-
607 blastoderm of w^{1118} as described in Siegal et al. (SIEGAL AND HARTL 2000). Adult flies
608 from injected embryos were backcrossed to w^{1118}, and the transgenes were
609 identified by the presence of eye pigment in the adult progenies. Transgenic flies
610 were next crossed with the double balancer (*Pin/CyO; TM2/TM6*) to know
611 chromosomes of P-element integration and making homozygous stock. We
612 established several lines for each predicted CBE and PRE (Supplementary Table 2-
613 4). The test fragment was flipped out from initial transgene, to compare the effect of
614 test fragment and rule out any position effect, by crossing the flies with *Cre-*
615 *recombinase* expressing flies and later was confirmed by PCR using specific
616 primers. The homozygous *ey*-dPRE males were crossed to virgin females of different
617 PcG proteins mutant (Pc^{1}, Psc^{1}, Pho^{1}) to investigate the effect on repressor function
618 of *ey*-dPRE (listed in Supplementary Table 6). The effect of PcG mutations effect
619 were compared in progenies with or without mutations in heterozygous condition.
620
621 ***Visualization and quantitative measurement of eye pigment***
622
623 The level of pigment in the eye of similar aged (5-day) adults were visually
624 determined to compare the level of *mini-white* expression in the enhancer-blocker
625 and PRE assay transgenic flies. In transgenic flies, pigmentation range varied
626 from bright/dark red in wild-type (*CS*) toward red, dark orange/light red, yellow,
627 and light-yellow, to white in the absence of expression (Supplementary Table 2-4).
628 We also quantitated the red pigment value in eye for some transgenic flies, to
629 compare the strength and effect of boundary and PRE after flipping-out (SULTANA *et*
630 *al.* 2011). Eye pigments from a minimum of ten adult heads were extracted in a 1:1
631 mixture of chloroform/0.1% ammonium hydroxide (200 µl) then, and centrifuged the
632 mix for 2 min at 13000 rpm. Finally, 100 µl of the supernatant was taken for
633 quantification of red pigment by spectrophotometric absorbance at 485 nm. A mean
634 relative pigmentation and standard error were calculated from a minimum of three
635 independent pigment values for each line by comparing it to the pigment value
636 of w^{1118}.
637
638 ***β-galactosidase staining and quantification***

For enhancer blocker assay in embryo, X-gal staining was performed to determine the beta-galactosidase (lacZ) activity (BELLEN *et al.* 1989; SULTANA *et al.* 2011). In brief, 0-12-h old embryos were collected and dechorionated in 50% bleach (sodium hypochlorite). The dechorionated embryos were washed and fixed for 20 min in heptane (saturated with 25% glutaraldehyde). The fixed embryos were again washed thoroughly with 1x PBST (0.3% Triton X-100), incubated initially for 10 min at 37^0C in X-gal staining solution (3 mM $K_3[Fe(CN)_6]$, 3 mM $K_4[Fe(CN)_6]$, 7.2 mM Na_2HPO_4, 2.8 mM NaH_2PO_4, 1 mM $MgCl_2$, 150 mM NaCl), and finally stained for 4-6 h in X-gal staining solution with 0.2% X-gal (Sigma). The stained embryos were imaged in Leica stereomicroscope. We performed X-gal staining of multiple transgenic lines along with positive and negative controls in a common grid, ensuring reliable comparison of staining between different genotypes.

To estimate and compare the enhancer blocker activity of the test fragments in the embryos, we quantitated X-gal staining using ImageJ-image processing and analysis software provided by the National Institutes of Health, USA (HARTIG 2013). We used pixels value of a fixed area size of different regions from multiple stained embryos of each genotype to calculate relative X-gal staining and standard error and plotted as a bar graph for comparison.

3C Assay

3C experiment was carried out in wild type *CS* embryos as described earlier (DEKKER *et al.* 2002; COMET *et al.* 2011) with few modifications. To begin with, 0-16 h old embryos (1 g) were dechorionated in 50% bleach for 5 min. The dechorionated embryos were washed thoroughly PBST (PBS 1x + 0.01% Triton X 100) and fixed for 15-20 min at room temperature (RT) with 2% formaldehyde (Sigma) in 5 ml fixing solution (50 mM HEPES-pH-7.6, 100 mM NaCl, 0.1 mM Na-EDTA-pH-8, 0.5 mM Na-EGTA-pH-8) added with 15 ml heptane. To stop fixation, formaldehyde was quenched by 0.125 M glycine for 5 min at RT. The fixed embryos were resuspended in 2.5 ml of ice-cold lysis buffer (10 mM Tris-pH-8, 10 mM NaCl, 0.2% NP40 with Roche protease inhibitor cocktail freshly added) and homogenized in Dounce homogenizer (10-15 strokes) to create nuclei suspension. Cellular debris was

removed from the nuclei suspension by filtration through a double layer of Mira cloth. Later, the nuclei were washed once with 500µl 1.2xNEB EcoRI buffer then resuspended in 500µl 1.2x NEB EcoRI buffer with 0.01% Triton X-100. A 50µl of nuclear solution (~100mg embryos) was lysed in 362µl 1.2x NEB EcoRI buffer with 1% SDS for 2 h at 37^0C. To stop the lysis triton X-100 was added to 0.01% and incubated for another 2 h at 37^0C. Subsequently, EcoRI digestion was carried out with 400 units of EcoRI (NEB) for 2h at 37^0C then inactivated the EcoRI at 65^0C for 20 min by adding SDS to a final concentration of 1.5 %. Afterwards, 1% Triton X-100 was added to neutralize the SDS at 37 ^{0}C for 1 h. EcoRI digested samples were diluted ten times in 1x NEB ligation buffer and ligated with 8µl ligase (400 U/*µl*, NEB) for 3-4 h at 22 ^{0}C. The ligated (3C) DNA was sequentially treated with RNaseA (20 µg/ml) for 30 minutes at 37 ^{0}C and with 100 µg/ml Proteinase-K at 55 ^{0}C for 1 h, and subsequently de-crosslinked overnight at 65 ^{0}C. Finally, 3C DNA was extracted by phenol: chloroform: isoamyl alcohol (25:24:1) and ethanol precipitation method. DNA from nuclei suspension and EcoRI digested samples were also prepared to compare the digestion and ligation efficiency.

The purified 3C DNA was used for PCR to check the interaction of different regions using all forward primers. Since we did not have a BAC clone available for *ey* region, we used forward-reverse primer pair to amplify regions flanking to selected restriction sites. These regions were mixed in an equimolar ratio, EcoRI restricted digested, and ligated. The randomly ligated product used to check the efficiency of the forward primer pairs. All PCRs amplifications were carried out with the following parameters: 95 ^{0}C for 3min, followed by 36 cycles of 95 ^{0}C- 30 s, 56 ^{0}C-10 s, and 72 ^{0}C-8 s, with a final step at 72 ^{0}C-2min. All forward primer pairs having similar amplification efficiency were next used for PCR amplification of 3C DNA. The 3C ligated PCR products were resolved on 1.2% agarose gel, and we confirmed the chimeric sequences by sequencing of gel extracted PCR DNA. The signal intensity of the 3C PCR product in the gel was quantified using ImageJ. Later, interaction frequency and standard deviations for each forward primer pairs were calculated from three replicates as described in Naumova et al. (NAUMOVA *et al.* 2012).

Analysis of HiC data from previous studies

To understand *ey* locus organization, we used the HiC data of embryos from Sexton et al. (SEXTON *et al.* 2012), in Kc167 cells from Eagen et al. (EAGEN *et al.* 2017), Li et al., and Cubenas et al. (LI *et al.* 2015; CUBENAS-POTTS *et al.* 2017). The processed HiC matrix data were used in two online visualization tools, i.e., Juicebox (ROBINSON *et al.* 2018) and HiCExplorer (WOLFF *et al.* 2018), to find out chromatin interactions.

Nuclear matrix Association Assay

The nuclear matrix (NuMat) association of *ey cis*-elements were tested in a modified *in vivo* MAR assay from the original protocol of Mirkovitch, *et al.* 1984 (MIRKOVITCH *et al.* 1984; PATHAK *et al.* 2014) (Supplementary Figure 3).

First, NuMat DNA was prepared from 0-16 h old embryos, eye-antennal discs (3rd instar larvae), and S2 cells. In brief, nuclei were isolated from 1 g of embryos and ~ 200 pairs of eye-antennal imaginal discs and $2x10^6$ S2 cells. An aliquot of nuclei was used for the isolation and estimation of total genomic DNA for quality control checks. Isolated nuclei were treated with DNaseI in nuclei isolation buffer (20 mM Tris-pH-7.4, 20 mM KCl, 70 mM NaCl, 10 mM $MgCl_2$, 0.12 5mM spermidine 1mM PMSF, 0.5% Triton-X 100, and 200µg/ml DNaseI) at 4 ^{0}C for 1 h to remove chromatin. Chromatin depleted nuclei were collected by centrifugation at 3000 x g for 10 minutes. Non-matrix proteins were extracted out from the nuclei with 0.4 M NaCl for 5 min in extraction buffer (10 mM Hepes-pH-7.5, 4 mM EDTA, 0.25 mM spermidine, 0.1 mM PMSF, 0.5% (v/v) triton X-100) and another 5 min with 2 M NaCl in the extraction buffer to get NuMat. The NuMat pellet was washed twice with wash buffer (1 mM Tris-pH-7.4, 20 mM KCl, 1 mM EDTA, 0.25 mM spermidine, 0.1 mM PMSF) then treated with RNaseA (20 µg/ml) for 30 minutes at 37 ^{0}C and with 100 µg/ml Proteinase-K at 55 ^{0}C for 1 h. Finally, NuMat DNA was obtained by phenol:chloroform:isoamylalcohol (25:24:1) and ethanol precipitation method. NuMat DNA was dissolved in DNase free water and quantified using Nano-drop. An equal amount of NuMat DNA isolated from different tissues was labeled with 32^P-dATP by the Random Primer Labeling method.

Next, all the test regions were PCR amplified from fly genomic DNA using specific primers listed in Supplementary Table 5. A known histone gene matrix-associated

region (HISMAR) was used as a positive control and an exonic sequence of BEAF-32 gene (BEAF CDS) was used as a random control. The controls were used to compare the relative NuMat associations. An equal amount (~ 400 ng) of all PCR products were resolved first on a 1.2% TAE agarose gel and then transferred to a positively charged nylon membrane using a capillary transfer method. The membrane was then subjected to a standard Southern hybridization using ^{32}P-dATP labeled NuMat DNA as described earlier (PATHAK *et al.* 2014). Finally, the hybridization signals were observed in Phosphor Molecular Imager (PMI) from (BIORAD). Relative association to NuMat and standard deviation for each region was calculated by signal intensity from three replicate blots using ImageJ (HARTIG 2013).

Competing interests

The authors declare that they have no competing interests.

Funding

Council of Scientific and Industrial Research (CSIR), India has funded this work, through JRF/SRF/RA fellowships to SV and research grants to RKM.

CRediT author contribution statement

Shreekant Verma: Investigation, Methodology, Visualization, Writing – original draft. **Rashmi U Pathak**: Investigation, Writing – review and editing. **Rakesh K Mishra**: Resources, Visualization, Supervision, Funding acquisition, Writing – review and editing.

Acknowledgements

We thank Welcome Bender for his discussion and sharing of Pc binding data in *ey* locus (not shown). We thank Yaser Payferman for his help in cloning for *ey*-PRE and A. Srinivasan for his helpful inputs in PRE predictions.

References

769 Adachi, Y., B. Hauck, J. Clements, H. Kawauchi, M. Kurusu *et al.*, 2003 Conserved cis-
770 regulatory modules mediate complex neural expression patterns of the eyeless gene
771 in the Drosophila brain. Mech Dev 120**:** 1113-1126.
772 Ahanger, S. H., A. Srinivasan, D. Vasanthi, Y. S. Shouche and R. K. Mishra, 2013 Conserved
773 boundary elements from the Hox complex of mosquito, Anopheles gambiae. Nucleic
774 Acids Res 41**:** 804-816.
775 Americo, J., M. Whiteley, J. L. Brown, M. Fujioka, J. B. Jaynes *et al.*, 2002 A complex array of
776 DNA-binding proteins required for pairing-sensitive silencing by a polycomb group
777 response element from the Drosophila engrailed gene. Genetics 160**:** 1561-1571.
778 Aoki, T., A. Sarkeshik, J. Yates and P. Schedl, 2012 Elba, a novel developmentally regulated
779 chromatin boundary factor is a hetero-tripartite DNA binding complex. Elife 1**:**
780 e00171.
781 Aoki, T., S. Schweinsberg, J. Manasson and P. Schedl, 2008 A stage-specific factor confers
782 Fab-7 boundary activity during early embryogenesis in Drosophila. Mol Cell Biol 28**:**
783 1047-1060.
784 Ayme-Southgate, A., J. Vigoreaux, G. Benian and M. L. Pardue, 1991 Drosophila has a
785 twitchin/titin-related gene that appears to encode projectin. Proc Natl Acad Sci U S A
786 88**:** 7973-7977.
787 Bantignies, F., C. Grimaud, S. Lavrov, M. Gabut and G. Cavalli, 2003 Inheritance of Polycomb-
788 dependent chromosomal interactions in Drosophila. Genes Dev 17**:** 2406-2420.
789 Bellen, H. J., C. J. O'Kane, C. Wilson, U. Grossniklaus, R. K. Pearson *et al.*, 1989 P-element-
790 mediated enhancer detection: a versatile method to study development in
791 Drosophila. Genes Dev 3**:** 1288-1300.
792 Blanton, J., M. Gaszner and P. Schedl, 2003 Protein:protein interactions and the pairing of
793 boundary elements in vivo. Genes Dev 17**:** 664-675.
794 Bonchuk, A., O. Maksimenko, O. Kyrchanova, T. Ivlieva, V. Mogila *et al.*, 2015 Functional role
795 of dimerization and CP190 interacting domains of CTCF protein in Drosophila
796 melanogaster. BMC Biol 13**:** 63.
797 Byrd, K., and V. G. Corces, 2003 Visualization of chromatin domains created by the gypsy
798 insulator of Drosophila. J Cell Biol 162**:** 565-574.
799 Cavalli, G., and R. Paro, 1998 The Drosophila Fab-7 chromosomal element conveys
800 epigenetic inheritance during mitosis and meiosis. Cell 93**:** 505-518.
801 Cherbas, L., A. Willingham, D. Zhang, L. Yang, Y. Zou *et al.*, 2011 The transcriptional diversity
802 of 25 Drosophila cell lines. Genome Res 21**:** 301-314.
803 Chintapalli, V. R., J. Wang and J. A. Dow, 2007 Using FlyAtlas to identify better Drosophila
804 melanogaster models of human disease. Nat Genet 39**:** 715-720.
805 Comet, I., B. Schuettengruber, T. Sexton and G. Cavalli, 2011 A chromatin insulator driving
806 three-dimensional Polycomb response element (PRE) contacts and Polycomb
807 association with the chromatin fiber. Proc Natl Acad Sci U S A 108**:** 2294-2299.
808 Cubenas-Potts, C., M. J. Rowley, X. Lyu, G. Li, E. P. Lei *et al.*, 2017 Different enhancer classes
809 in Drosophila bind distinct architectural proteins and mediate unique chromatin
810 interactions and 3D architecture. Nucleic Acids Res 45**:** 1714-1730.
811 Czerny, T., G. Halder, U. Kloter, A. Souabni, W. J. Gehring *et al.*, 1999 twin of eyeless, a
812 second Pax-6 gene of Drosophila, acts upstream of eyeless in the control of eye
813 development. Mol Cell 3**:** 297-307.
814 Dekker, J., K. Rippe, M. Dekker and N. Kleckner, 2002 Capturing chromosome conformation.
815 Science 295**:** 1306-1311.

816 Desplan, C., 1997 Eye development: governed by a dictator or a junta? Cell 91: 861-864.
817 Dreos, R., G. Ambrosini, R. C. Perier and P. Bucher, 2015 The Eukaryotic Promoter Database:
818 expansion of EPDnew and new promoter analysis tools. Nucleic Acids Res 43: D92-
819 96.
820 Eagen, K. P., E. L. Aiden and R. D. Kornberg, 2017 Polycomb-mediated chromatin loops
821 revealed by a subkilobase-resolution chromatin interaction map. Proc Natl Acad Sci
822 U S A 114: 8764-8769.
823 Frise, E., A. S. Hammonds and S. E. Celniker, 2010 Systematic image-driven analysis of the
824 spatial Drosophila embryonic expression landscape. Mol Syst Biol 6: 345.
825 Fyrberg, C. C., S. Labeit, B. Bullard, K. Leonard and E. Fyrberg, 1992 Drosophila projectin:
826 relatedness to titin and twitchin and correlation with lethal(4) 102 CDa and bent-
827 dominant mutants. Proc Biol Sci 249: 33-40.
828 Gambetta, M. C., and E. E. M. Furlong, 2018 The Insulator Protein CTCF Is Required for
829 Correct Hox Gene Expression, but Not for Embryonic Development in Drosophila.
830 Genetics 210: 129-136.
831 Gaszner, M., and G. Felsenfeld, 2006 Insulators: exploiting transcriptional and epigenetic
832 mechanisms. Nat Rev Genet 7: 703-713.
833 Gerasimova, T. I., and V. G. Corces, 2001 Chromatin insulators and boundaries: effects on
834 transcription and nuclear organization. Annu Rev Genet 35: 193-208.
835 Geyer, P. K., C. Spana and V. G. Corces, 1986 On the molecular mechanism of gypsy-induced
836 mutations at the yellow locus of Drosophila melanogaster. EMBO J 5: 2657-2662.
837 Hagstrom, K., M. Muller and P. Schedl, 1996 Fab-7 functions as a chromatin domain
838 boundary to ensure proper segment specification by the Drosophila bithorax
839 complex. Genes Dev 10: 3202-3215.
840 Halder, G., P. Callaerts, S. Flister, U. Walldorf, U. Kloter *et al.*, 1998 Eyeless initiates the
841 expression of both sine oculis and eyes absent during Drosophila compound eye
842 development. Development 125: 2181-2191.
843 Hartig, S. M., 2013 Basic image analysis and manipulation in ImageJ. Curr Protoc Mol Biol
844 Chapter 14: Unit14 15.
845 Hauck, B., W. J. Gehring and U. Walldorf, 1999 Functional analysis of an eye specific
846 enhancer of the eyeless gene in Drosophila. Proc Natl Acad Sci U S A 96: 564-569.
847 He, B., C. Chen, L. Teng and K. Tan, 2014 Global view of enhancer-promoter interactome in
848 human cells. Proc Natl Acad Sci U S A 111: E2191-2199.
849 Hou, C., L. Li, Z. S. Qin and V. G. Corces, 2012 Gene density, transcription, and insulators
850 contribute to the partition of the Drosophila genome into physical domains. Mol Cell
851 48: 471-484.
852 Kassis, J. A., 1994 Unusual properties of regulatory DNA from the Drosophila engrailed gene:
853 three "pairing-sensitive" sites within a 1.6-kb region. Genetics 136: 1025-1038.
854 Kassis, J. A., 2002 Pairing-sensitive silencing, polycomb group response elements, and
855 transposon homing in Drosophila. Adv Genet 46: 421-438.
856 Kassis, J. A., and J. L. Brown, 2013 Polycomb group response elements in Drosophila and
857 vertebrates. Adv Genet 81: 83-118.
858 Kellum, R., and P. Schedl, 1991 A position-effect assay for boundaries of higher order
859 chromosomal domains. Cell 64: 941-950.
860 Lanzuolo, C., V. Roure, J. Dekker, F. Bantignies and V. Orlando, 2007 Polycomb response
861 elements mediate the formation of chromosome higher-order structures in the
862 bithorax complex. Nat Cell Biol 9: 1167-1174.

863 Li, L., X. Lyu, C. Hou, N. Takenaka, H. Q. Nguyen *et al.*, 2015 Widespread rearrangement of
864 3D chromatin organization underlies polycomb-mediated stress-induced silencing.
865 Mol Cell 58**:** 216-231.
866 Lin, N., X. Li, K. Cui, I. Chepelev, F. Tie *et al.*, 2011 A barrier-only boundary element delimits
867 the formation of facultative heterochromatin in Drosophila melanogaster and
868 vertebrates. Mol Cell Biol 31**:** 2729-2741.
869 Lo, P. C., and M. Frasch, 1999 Sequence and expression of myoglianin, a novel Drosophila
870 gene of the TGF-beta superfamily. Mech Dev 86**:** 171-175.
871 Maeda, R. K., and F. Karch, 2006 The ABC of the BX-C: the bithorax complex explained.
872 Development 133**:** 1413-1422.
873 Maroto, M., J. Vinos, R. Marco and M. Cervera, 1992 Autophosphorylating protein kinase
874 activity in titin-like arthropod projectin. J Mol Biol 224**:** 287-291.
875 Matzat, L. H., R. K. Dale, N. Moshkovich and E. P. Lei, 2012 Tissue-specific regulation of
876 chromatin insulator function. PLoS Genet 8**:** e1003069.
877 Mihaly, J., S. Barges, L. Sipos, R. Maeda, F. Cleard *et al.*, 2006 Dissecting the regulatory
878 landscape of the Abd-B gene of the bithorax complex. Development 133**:** 2983-2993.
879 Mirkovitch, J., M. E. Mirault and U. K. Laemmli, 1984 Organization of the higher-order
880 chromatin loop: specific DNA attachment sites on nuclear scaffold. Cell 39**:** 223-232.
881 Mishra, R. K., and F. Karch, 1999 Boundaries that demarcate structural and functional
882 domains of chromatin. Journal of Biosciences 24**:** 377-399.
883 Mishra, R. K., J. Mihaly, S. Barges, A. Spierer, F. Karch *et al.*, 2001 The iab-7 polycomb
884 response element maps to a nucleosome-free region of chromatin and requires both
885 GAGA and pleiohomeotic for silencing activity. Mol Cell Biol 21**:** 1311-1318.
886 mod, E. C., S. Roy, J. Ernst, P. V. Kharchenko, P. Kheradpour *et al.*, 2010 Identification of
887 functional elements and regulatory circuits by Drosophila modENCODE. Science 330**:**
888 1787-1797.
889 Naumova, N., E. M. Smith, Y. Zhan and J. Dekker, 2012 Analysis of long-range chromatin
890 interactions using Chromosome Conformation Capture. Methods 58**:** 192-203.
891 Negre, N., C. D. Brown, P. K. Shah, P. Kheradpour, C. A. Morrison *et al.*, 2010 A
892 comprehensive map of insulator elements for the Drosophila genome. PLoS Genet 6**:**
893 e1000814.
894 Ogiyama, Y., B. Schuettengruber, G. L. Papadopoulos, J. M. Chang and G. Cavalli, 2018
895 Polycomb-Dependent Chromatin Looping Contributes to Gene Silencing during
896 Drosophila Development. Mol Cell 71**:** 73-88 e75.
897 Pathak, R. U., N. Rangaraj, S. Kallappagoudar, K. Mishra and R. K. Mishra, 2007 Boundary
898 element-associated factor 32B connects chromatin domains to the nuclear matrix.
899 Mol Cell Biol 27**:** 4796-4806.
900 Pathak, R. U., A. Srinivasan and R. K. Mishra, 2014 Genome-wide mapping of matrix
901 attachment regions in Drosophila melanogaster. BMC Genomics 15**:** 1022.
902 Pichaud, F., and C. Desplan, 2001 A new visualization approach for identifying mutations
903 that affect differentiation and organization of the Drosophila ommatidia.
904 Development 128**:** 815-826.
905 Quiring, R., U. Walldorf, U. Kloter and W. J. Gehring, 1994 Homology of the eyeless gene of
906 Drosophila to the Small eye gene in mice and Aniridia in humans. Science 265**:** 785-
907 789.

908 Robinson, J. T., D. Turner, N. C. Durand, H. Thorvaldsdottir, J. P. Mesirov *et al.*, 2018
909 Juicebox.js Provides a Cloud-Based Visualization System for Hi-C Data. Cell Syst 6**:**
910 256-258 e251.
911 Ronshaugen, M., and M. Levine, 2004 Visualization of trans-homolog enhancer-promoter
912 interactions at the Abd-B Hox locus in the Drosophila embryo. Dev Cell 7**:** 925-932.
913 Sexton, T., F. Bantignies and G. Cavalli, 2009 Genomic interactions: chromatin loops and
914 gene meeting points in transcriptional regulation. Semin Cell Dev Biol 20**:** 849-855.
915 Sexton, T., E. Yaffe, E. Kenigsberg, F. Bantignies, B. Leblanc *et al.*, 2012 Three-dimensional
916 folding and functional organization principles of the Drosophila genome. Cell 148**:**
917 458-472.
918 Siegal, M. L., and D. L. Hartl, 2000 Application of Cre/loxP in Drosophila. Site-specific
919 recombination and transgene coplacement. Methods Mol Biol 136**:** 487-495.
920 Sigrist, C. J., and V. Pirrotta, 1997 Chromatin insulator elements block the silencing of a
921 target gene by the Drosophila polycomb response element (PRE) but allow trans
922 interactions between PREs on different chromosomes. Genetics 147**:** 209-221.
923 Srinivasan, A., and R. K. Mishra, 2012 Chromatin domain boundary element search tool for
924 Drosophila. Nucleic Acids Res 40**:** 4385-4395.
925 Srinivasan, A., and R. K. Mishra, 2020 Genomic organization of Polycomb Response Elements
926 and its functional implication in Drosophila and other insects. J Biosci 45.
927 Sultana, H., S. Verma and R. K. Mishra, 2011 A BEAF dependent chromatin domain boundary
928 separates myoglianin and eyeless genes of Drosophila melanogaster. Nucleic Acids
929 Res 39**:** 3543-3557.
930 Thomas, S., X. Y. Li, P. J. Sabo, R. Sandstrom, R. E. Thurman *et al.*, 2011 Dynamic
931 reprogramming of chromatin accessibility during Drosophila embryo development.
932 Genome Biol 12**:** R43.
933 Valenzuela, L., and R. T. Kamakaka, 2006 Chromatin insulators. Annu Rev Genet 40**:** 107-138.
934 Vasanthi, D., A. Nagabhushan, N. K. Matharu and R. K. Mishra, 2013 A functionally
935 conserved Polycomb response element from mouse HoxD complex responds to
936 heterochromatin factors. Sci Rep 3**:** 3011.
937 Vogelmann, J., A. Le Gall, S. Dejardin, F. Allemand, A. Gamot *et al.*, 2014 Chromatin insulator
938 factors involved in long-range DNA interactions and their role in the folding of the
939 Drosophila genome. PLoS Genet 10**:** e1004544.
940 Wang, Q., Q. Sun, D. M. Czajkowsky and Z. Shao, 2018 Sub-kb Hi-C in D. melanogaster
941 reveals conserved characteristics of TADs between insect and mammalian cells. Nat
942 Commun 9**:** 188.
943 West, A. G., M. Gaszner and G. Felsenfeld, 2002 Insulators: many functions, many
944 mechanisms. Genes Dev 16**:** 271-288.
945 Wolff, J., V. Bhardwaj, S. Nothjunge, G. Richard, G. Renschler *et al.*, 2018 Galaxy HiCExplorer:
946 a web server for reproducible Hi-C data analysis, quality control and visualization.
947 Nucleic Acids Res 46**:** W11-W16.
948 Wolle, D., F. Cleard, T. Aoki, G. Deshpande, P. Schedl *et al.*, 2015 Functional Requirements
949 for Fab-7 Boundary Activity in the Bithorax Complex. Mol Cell Biol 35**:** 3739-3752.
950 Zhang, Y., C. H. Wong, R. Y. Birnbaum, G. Li, R. Favaro *et al.*, 2013 Chromatin connectivity
951 maps reveal dynamic promoter-enhancer long-range associations. Nature 504**:** 306-
952 310.
953

954

Figure legends

Figure 1. CBE prediction at the *ey* locus. (a) (i) *ey* locus with flanking genes *myo* and *bt* in the fourth chromosome in *Drosophila melanogaster* (genome version dm3). **(ii)** Mapping of the boundary proteins binding sites and DHS. Embryonic (0-12 h) ChIP-chip binding data of BEAF-32, CP190, CTCF, and GAF are used from Negre et al. (NEGRE *et al.* 2010). For DHS mapping embryonic stage 9 (~6 h) DHS data from Thomas et al. is used (THOMAS *et al.* 2011). **(iii)** Predicted CBEs. CdBEST predicts previously reported ME between *ey* and *myo* and INT7 in the seventh intronic region of *ey*. Additionally, boundary protein bindings and DHS coincide with INT7(~1.2 Kb) and EB (~2.2 Kb) genomic regions (highlighted in light green). **(b)** Detailed mapping of boundary proteins binding peaks (BEAF-32, CTCF and CP190) and DHS in INT7 and EB region that are tested for enhancer blockers. CTCF binding and DHS at EB present in two sites EB-u and EB-i.

Figure 2. EB functions as Enhancer blocker adult eye (a) Enhancer blocker assay construct, pRW$^+$. The test fragment flanking with *loxP* sites is inserted between the enhancer and promoter of *mini-white*. **(b)** Enhancer blocker assay in the eye. Eye color comparisons of RW$^+$ transgenes. In each panel, the eye on the left contains the test fragment in heterozygous (P/+), whereas the eye on the right is the same line after the fragment is flipped out (ΔP/+). INT7 region does not show enhancer blocker activity while EB shows a weak enhancer blocker activity. EB-u and EB-i, when tested separately, only EB-i shows similar activity to EB suggest the boundary function of EB resides in EB-i. The graph represents the relative pigment value in the eye. An average mean and standard error in bars is calculated from a minimum of 10 eyes in triplicates.

Figure 3. EB functions as an Enhancer blocker in the embryo. (a) Enhancer blocker assay construct, pCfhL. If a test DNA, inserted between the *ftz* enhancers and *hsp70*/*lacZ* gene, functions as a boundary, it prevents the enhancer from driving the reporter gene, thereby, giving the low intensity of X-gal staining, which restore upon flipping out the test DNA and enhance the staining. **(b**) LacZ/X-gal staining of the embryos. The panel compares the x-gal staining during early development (UPS mediated) of the initial (P/P) and flipped-out (ΔP/ΔP) transgenes of INT7, EB, EB-u,

and EB-i. The pCfhL construct alone and with Fab7 boundary used as negative and positive controls, respectively. INT7 in shows a weak enhancer blocker effect while EB shows a significant enhancer blocking activity. Further, the boundary activity of EB resides in EB-i, whereas EB-u does not show enhancer blocker effect. **(c)** Quantification LacZ staining. The relative x-gal staining and standard errors are calculated from multiple stained embryos using the ImageJ software.

Figure 4. PRE prediction in *ey* locus. (a) Regulatory elements at *ey* locus. Known enhancers (orange) of *ey* identified in previous studies which have shown *ey* specific enhancer activity are present at upstream, i.e., *ey_12E* and in the second intron, i.e., *ey_3.6R* and *ey_D02* (HAUCK *et al.* 1999; ADACHI *et al.* 2003). The two boundaries, ME and EB, demarcate the *ey* locus. Two *ey* promoters, *ey_1* and *ey_2* predicted in *ey* locus at eukaryotic promoter database (DREOS *et al.* 2015). **(b)** A ~1.6kb *ey*-PRE and a core 831bp *ey*-dPRE in *ey* locus predicted by PRE mapper. The *ey* promoter *ey_2* also coincide with *ey*-PRE. **(c)** Mapping of histone modifications, binding sites of PcG and boundary proteins, and DHS at *ey* locus in the 14-16h whole embryo. H3K27Ac (blue), H3K27Me3 (red), Pc (purple), dRING(brown), Psc(green), boundary proteins (black), and DHS(orange). ChIP-seq data from the modENCODE project (MOD *et al.* 2010) and DHS data of stage 9 (~6h) embryo from Thomas et al. 2011 (THOMAS *et al.* 2011) study have been used at the UCSC browser to generate the map. The *ey* locus has a repressed H3K27Me3 domain, whereas neighboring genes *myo* and *bt* both have active H3K27Ac marks at their promoters. The binding of Pc spreads over the repressed domain of *ey* while dRING, and Psc, along with Pc, show a sharp peak at upstream to the first exon. The *ey*-PRE aligns with the strong peak of PcG proteins, and core *ey*-dPRE maps to DHS. Boundary proteins BEAF-32, CP190, and CTCF bind at both ME and EB that appear to delimit the repressed domain of *ey*.

Figure 5. Functional validation of *ey*-PRE (a) A PRE assay vector pCasPeRX. The test DNA is inserted upstream to a *mini-white*. If the test DNA is PRE, it causes repression of *mini-white*. The test fragments later can be removed with the help of *loxP* to confirm the PRE mediated repression activity and rule out any position effect of the genomic environment. **(b)** *ey*-PREs function as a repressor and show strong PSS. Both, *ey*-PRE (~1.6kb) and *ey*-dPRE (831bp) exhibit stronger

repression in of *mini-white* in homozygous (P/P) compared to their heterozygotes (P/+). The flipped-out versions of the same (ΔP/+ and ΔP/ΔP) show the de-repression of *mini-white*. More than 50% of *ey*-PREs lines show intense repression of *mini-white* represented by very light and variegating eye color. The smaller version *ey*-dPRE show repression activity to a similar extent suggests that smaller fragment is sufficient for the PRE activity (see Table1 and supplementary table 4). **(c)** Effect of PcG mutations on *ey*-PRE. All eyes are heterozygous for *ey*-PRE and PcG mutations. The graph represents a quantitative analysis of the eye color in the heterozygous condition in wild type and different PcG proteins mutation background. PcG mutations, Pc^1 and Pho^1 both show a mild de-repression effect while Psc^1 attenuates the *ey*-dPRE function significantly (see Table 2). Mutation in GAF (Trl^{R85}) also attenuates the PRE repressor effect. A double PcG mutation of Pc^1 and Psc^1 show accumulative de-repressions effect.

Figure 6. ME, EB, and *ey*-PRE interact in long-range to regulate *ey* locus. **(a)** Interaction of ME with various regions at *ey* locus. 3C was performed in the 0-16h embryo using EcoRI restrictions digestion followed by ligation, then Ligated hybrids were PCR amplified using all forward primer pairs and confirmed by sequencing. Interaction frequencies mean and standard deviations (b-vi) were calculated by gel quantification of three replicates, as described (NAUMOVA *et al.* 2012). EcoRI fragment that contains ME (primer 1) interacts with *ey*-PRE (primer 3) and with an internal region (primer 4) and EB (primer 6) of *ey* (red lines in b-vi). However, such interactions are not observed in a nearby upstream region towards *myo* (primer -3, -2 and -1), a few internal regions of *ey* (primer 2 and 5) and in farther downstream regions of *bt* (primer 7 and 8) (grey lines in a-vi). **(b)** Comparative analysis of chromatin interaction at *ey* locus. (i & II) A merge Hi-C heatmap of chromatin interactions in ~250 kb region of the fourth chromosome along with genes in Kc cells. HiC data from Li et al. & Cubenas et al. (LI *et al.* 2015; CUBENAS-POTTS *et al.* 2017) visualized using HiC-Explorer (WOLFF *et al.* 2018) and chromatin loops inferred from the same (shaded triangles). (iii) Interaction map in *ey* region inferred from the enhancer-promoter interaction study used in an integrated method for predicting enhancer targets (IM-PET) available from 4Dgenome (https://4dgenome.research.chop.edu/) (HE *et al.* 2014) (iv) Genes and regulatory region of *ey*. (v) EcoRI sites and forward primers used for 3C. (vi) & (vii) ME

interacting regions and interaction frequencies in the embryo identified by 3C in this study. Together 3C and HiC data suggest ME and EB interacts in long range to demarcates the ey domain.

Figure 7. Different regions of eyeless associate to NuMat. (a) A map of *ey* locus along with NuMat association of *cis*-elements ME, *ey*-dPRE, EB-u, and EB-i. **(b)** NuMat association of *ey cis*-elements along with known MAR (histone MAR region – HIS MAR) as a +ve and BEAF coding sequence (BEAF CDS) as a -ve control. The PCR products of test and controls DNA (~400ng) were electrophoresed on 1% agarose gel, transferred to the NY+ membrane. Finally, southern hybridized with radiolabeled NuMat DNA from the embryos (0-16h), brain-eye-antennal disc (3rd instar larvae), and S2 cells. **(C)** Relative NuMat association of all the test region is compared with BEAF CDS (considered as one in embryos) and calculated by blot/gel quantification using ImageJ. *Ey*-dPRE and EB-u show a strong NuMat association (comparable to HIS MAR) in the embryo and brain-eye-antennal disc. ME and EB-i show similar weak interaction to the matrix in the embryos while in brain-eye-antennal disc EB-i does not appear to interact with the matrix. In S2 cells, only e*y*-dPRE associates with the matrix whereas in all experiment INT7 does not interact NuMat (comparable to BEAF CDS).

Figure 8. A Model for regulation of *eyeless* locus. Gene regulation in cells is a result of a spatio-temporal higher-order organization of the chromatin. *Cis*-regulatory elements aid in tethering of a locus into a needed sub-nuclear compartment, at least in some regions, by attaching to the nuclear matrix. In the absence of activation signal by initial regulatory proteins or upon receiving a repressive signal during development, PcG proteins bind to *ey*-PRE to bring and maintain transcriptional repression of *ey*. As *ey* and *bt* are present in a common TAD (Figure 6b) in Kc cells where both the genes are transcriptionally inactive It is likely that *ey* and *bt* are in the same repressed domain. Further, the *ey*-PRE tethering to the matrix and the chromatin interactions of ME with *ey*-PRE, EB, and downstream regions of the *bt* collectively determine the higher-order chromatin organization at the repressed domain(**i**). While upon activation signal during development, the *ey* gene moves out into an active compartment of the nucleus likely with the help of *ey*-PRE as it associates to NuMat in all tissues (**ii**). Moreover, *ey* promoter that coincides with *ey*-

PRE becomes a target of activators, i.e., trxG proteins and enhancer proteins that

	***ey*-PRE**	***ey*-dPRE**
Total number of lines	31	26
% lines variegating	58 (18/31)	21 (4/19)
% lines with light eye color	52 (16/31)	50 (13/26)
% lines showing PSS	32 (7/22)	36 (5/14)
% lines showing increase in eye color in flipped-outs	59 (16/27)	47(8/17)

keep *ey* active. At the same time, ME and EB boundaries demarcate the independent domain of *ey* that restrict cross-regulatory influences with neighboring genes *myo* and *bt.*

Table 1: *ey*-PRE and *ey*-dPRE transgenes repressor activity

Table 2: PcG mutations effect on *ey*-PRE mediated repression

***ey*-PRE lines**	**PcG Mutation**	**Effect**	**Strength**
13.2	Pc^1	Derepression	+
	Psc^1	Derepression	++
	Pho^1	Derepression	+
	Trl^{R85}	Derepression	++
	$Pc^1;Psc^1$	Derepression	+++
76.1	Pc^1	No effect	
	Psc^1	Derepression	++
	Pho^1	No effect	
	Trl^{R85}	Derepression	++
	$Pc^1; Psc^1$	Derepression	++
100.2	Pc^1	Derepression	+
	Psc^1	Derepression	++
	Pho^1	Derepression	+
	Trl^{R85}	Derepression	++
	$Pc^1; Psc^1$		
88.1	Pc^1	Derepression	+
	Psc^1	Derepression	++
	Pho^1	Derepression	+
	Trl^{R85}	Derepression	++

	Pc^{1}; *Psc*^{1}	Derepression	+++
10.2	*Pc*^{1}	No effect	
	Psc^{1}	Derepression	++
	Pho^{1}	Derepression	+
	Trl^{R85}	Derepression	++
	Pc^{1}; *Psc*^{1}	Derepression	+++

Figure 1

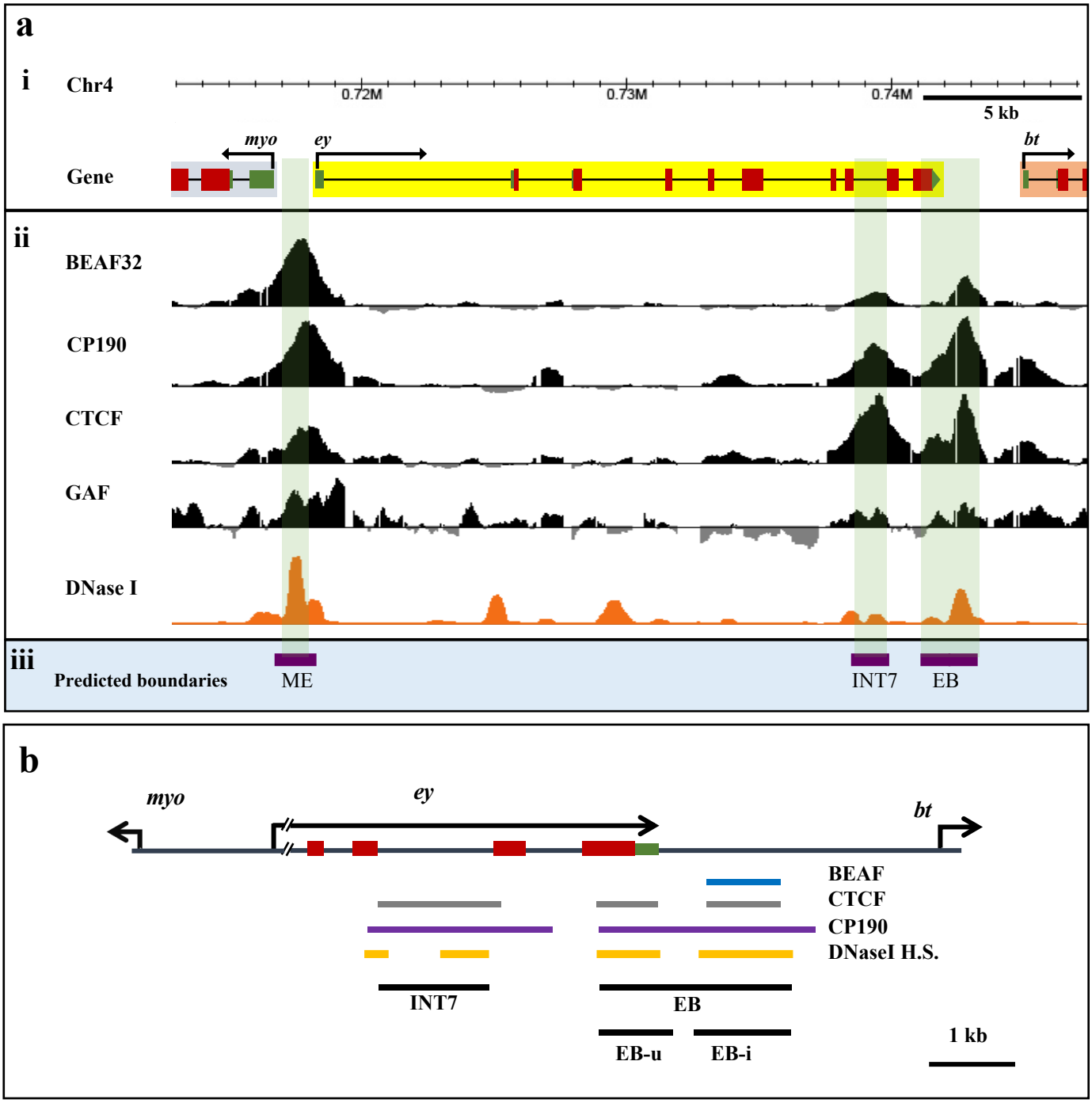
a
i
Chr4
0.72M
0.73M
0.74M
5 kb
Gene
myo
ey
bt
ii
BEAF32
CP190
CTCF
GAF
DNase I
iii
Predicted boundaries
ME
INT7
EB
b
myo
ey
bt
BEAF
CTCF
CP190
DNaseI H.S.
INT7
EB
EB-u
EB-i
1 kb

Figure 2

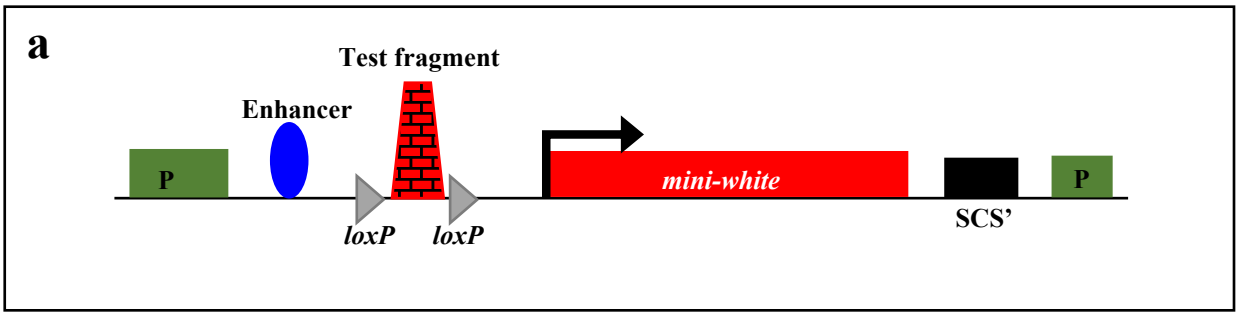
a
Test fragment
Enhancer
P
loxP
loxP
mini-white
SCS'
P

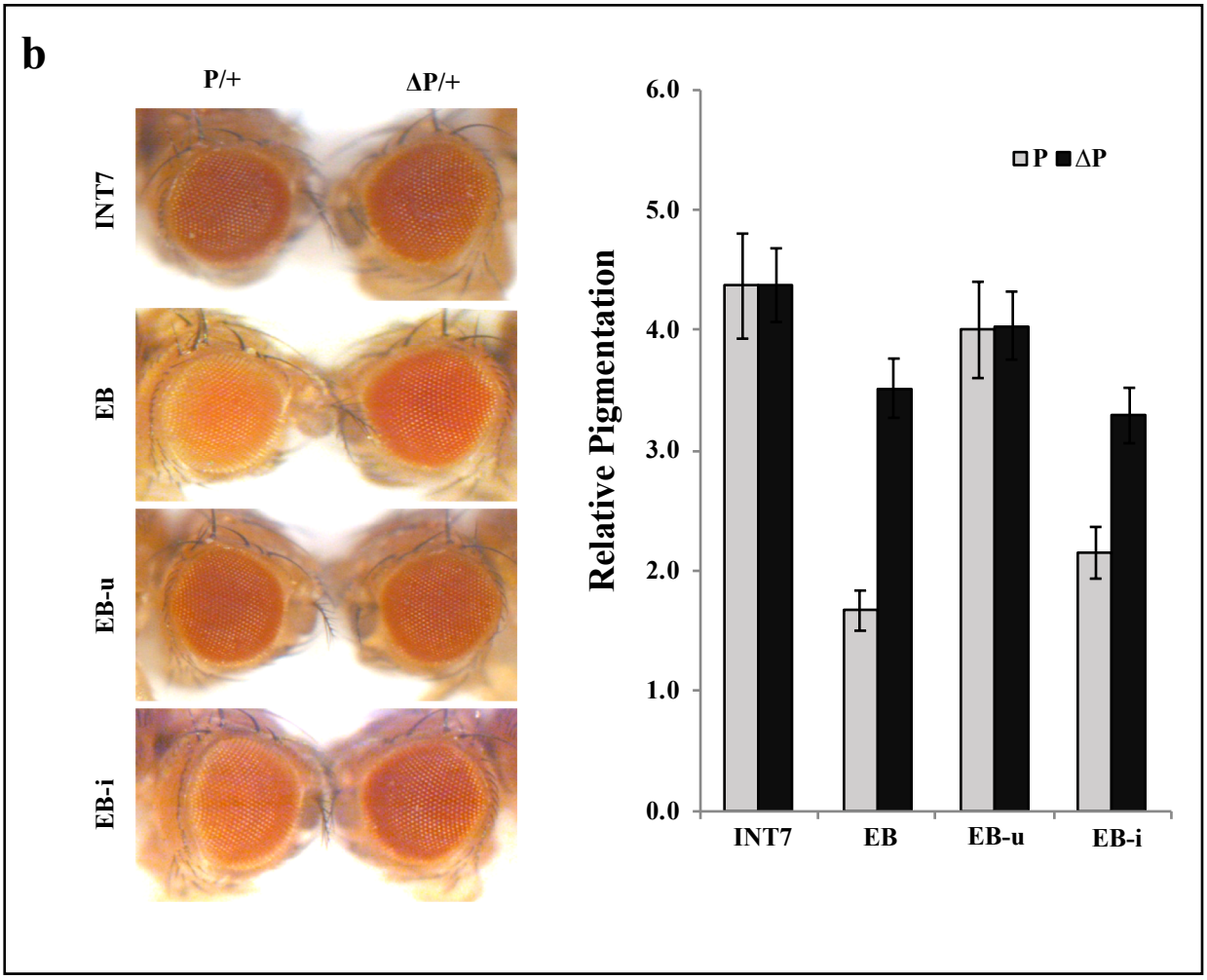
b
P/+
ΔP/+
INT7
EB
EB-u
EB-i
Relative Pigmentation
6.0
5.0
4.0
3.0
2.0
1.0
0.0
P
ΔP
INT7
EB
EB-u
EB-i

Figure 3

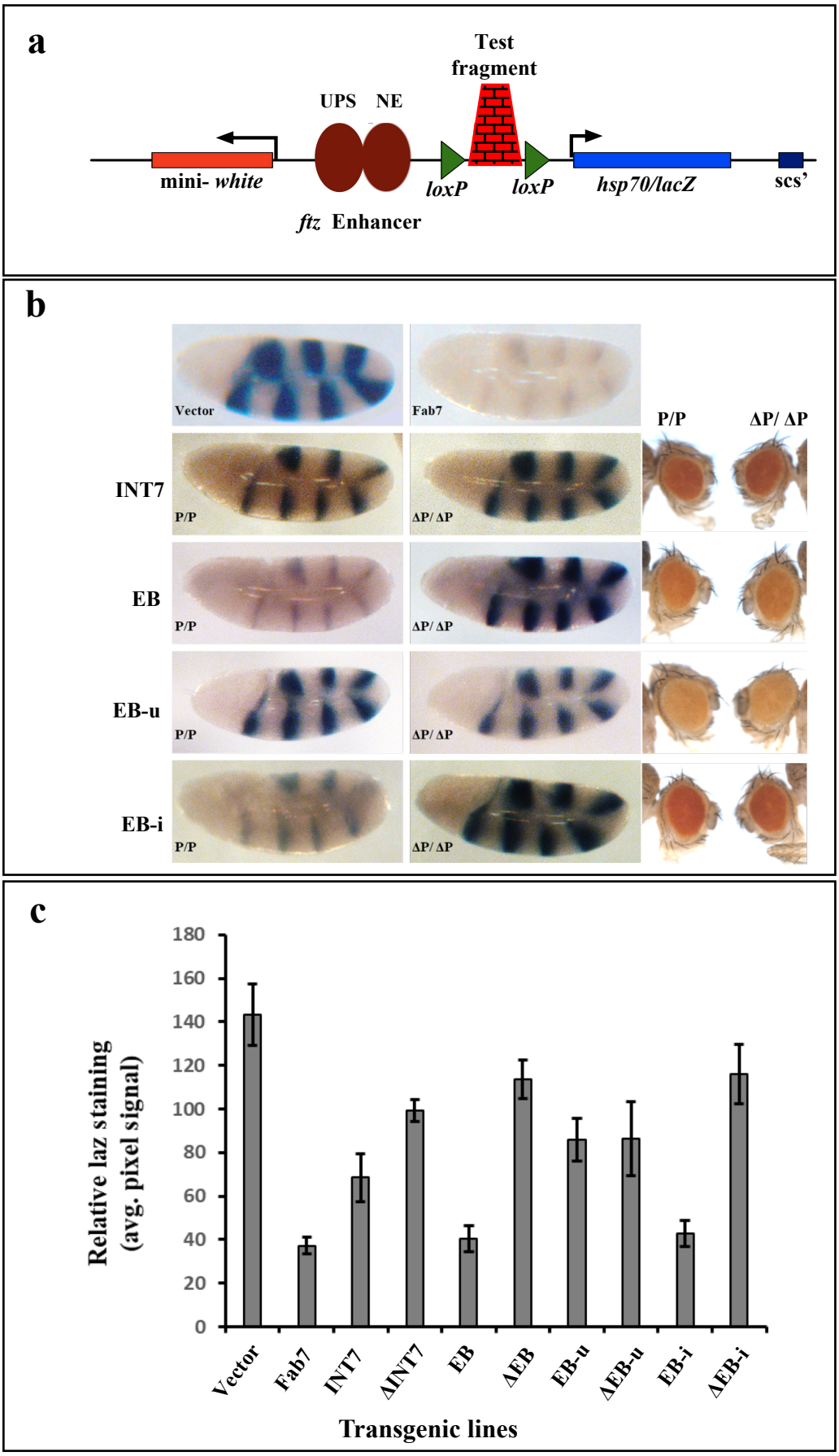
a
Test fragment
UPS
NE
mini- white
loxP
loxP
hsp70/lacZ
scs'
ftz Enhancer
b
Vector
Fab7
P/P
ΔP/ ΔP
INT7
EB
EB-u
EB-i
P/P
ΔP/ ΔP
c
Relative laz staining (avg. pixel signal)
180
160
140
120
100
80
60
40
20
0
Vector
Fab7
INT7
ΔINT7
EB
ΔEB
EB-u
ΔEB-u
EB-i
ΔEB-i
Transgenic lines

Figure 4

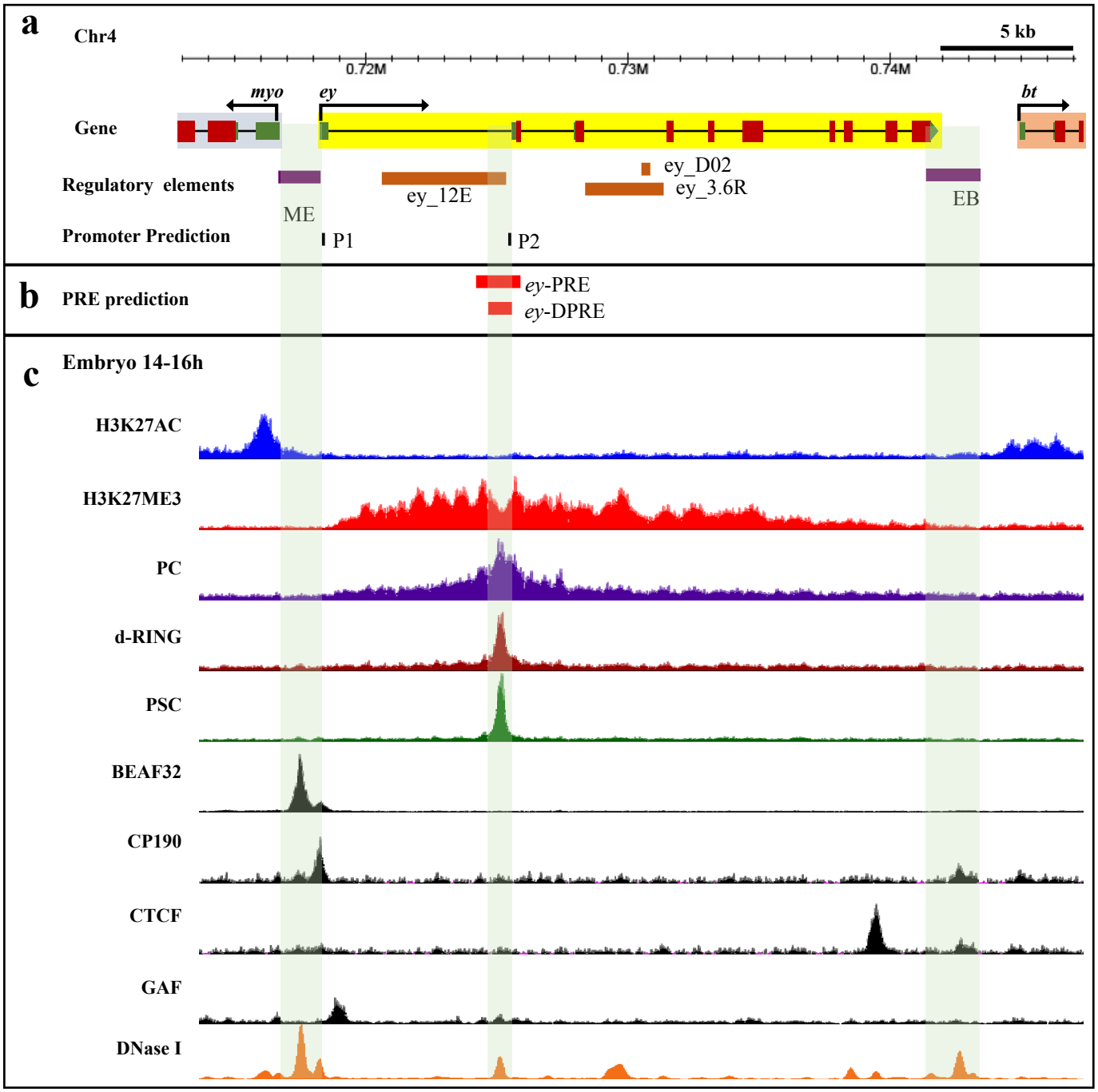
a
Chr4
5 kb
0.72M
0.73M
0.74M
myo
ey
bt
Gene
Regulatory elements
ey_D02
ey_12E
ey_3.6R
ME
EB
Promoter Prediction
P1
P2
b
PRE prediction
ey-PRE
ey-DPRE
c
Embryo 14-16h
H3K27AC
H3K27ME3
PC
d-RING
PSC
BEAF32
CP190
CTCF
GAF
DNase I

Figure 5

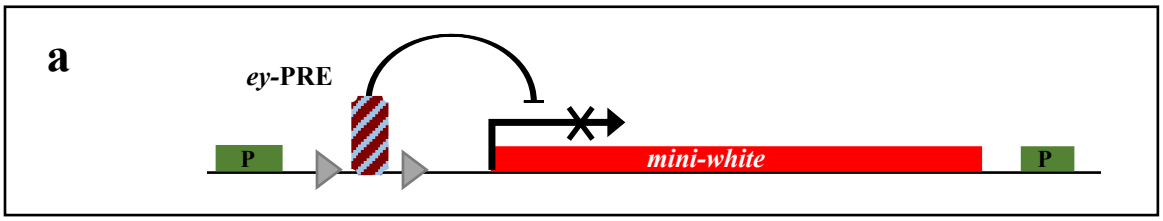
a
ey-PRE
P
mini-white
P

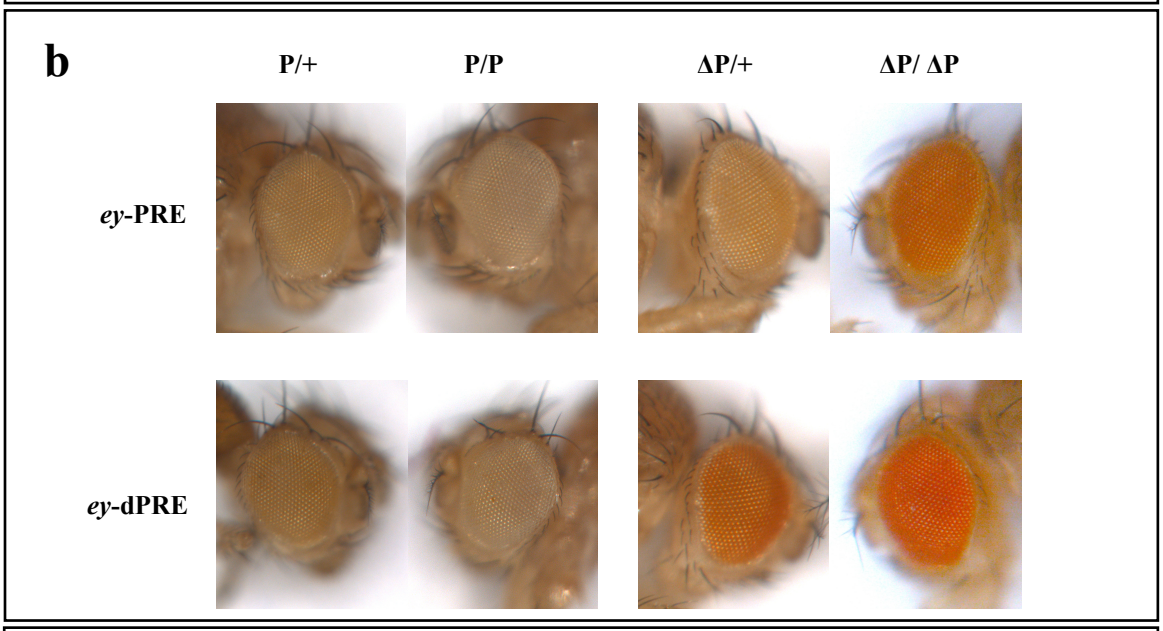
b
P/+
P/P
ΔP/+
ΔP/ ΔP
ey-PRE
ey-dPRE

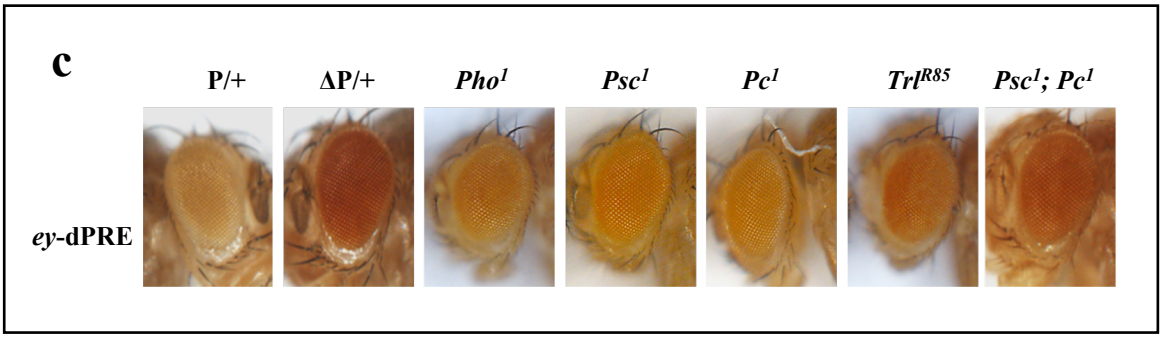
c
P/+
ΔP/+
Pho1
Psc1
Pc1
TrlR85
Psc1; Pc1
ey-dPRE

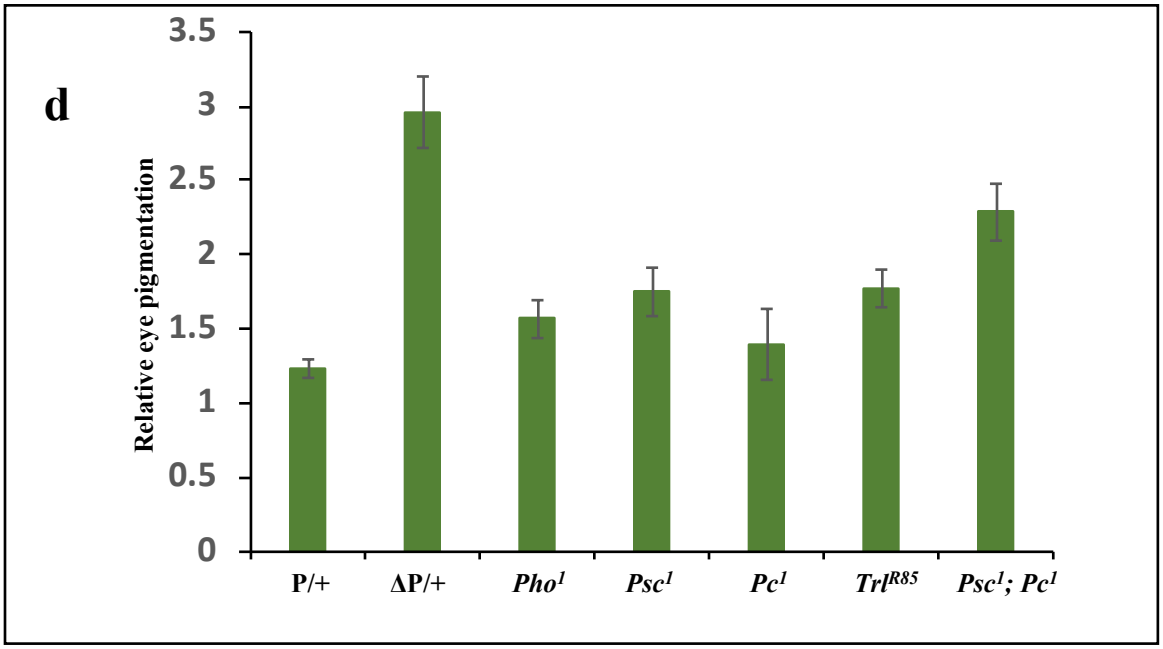
d
Relative eye pigmentation
3.5
3
2.5
2
1.5
1
0.5
0
P/+
ΔP/+
Pho1
Psc1
Pc1
TrlR85
Psc1; Pc1

Figure 6

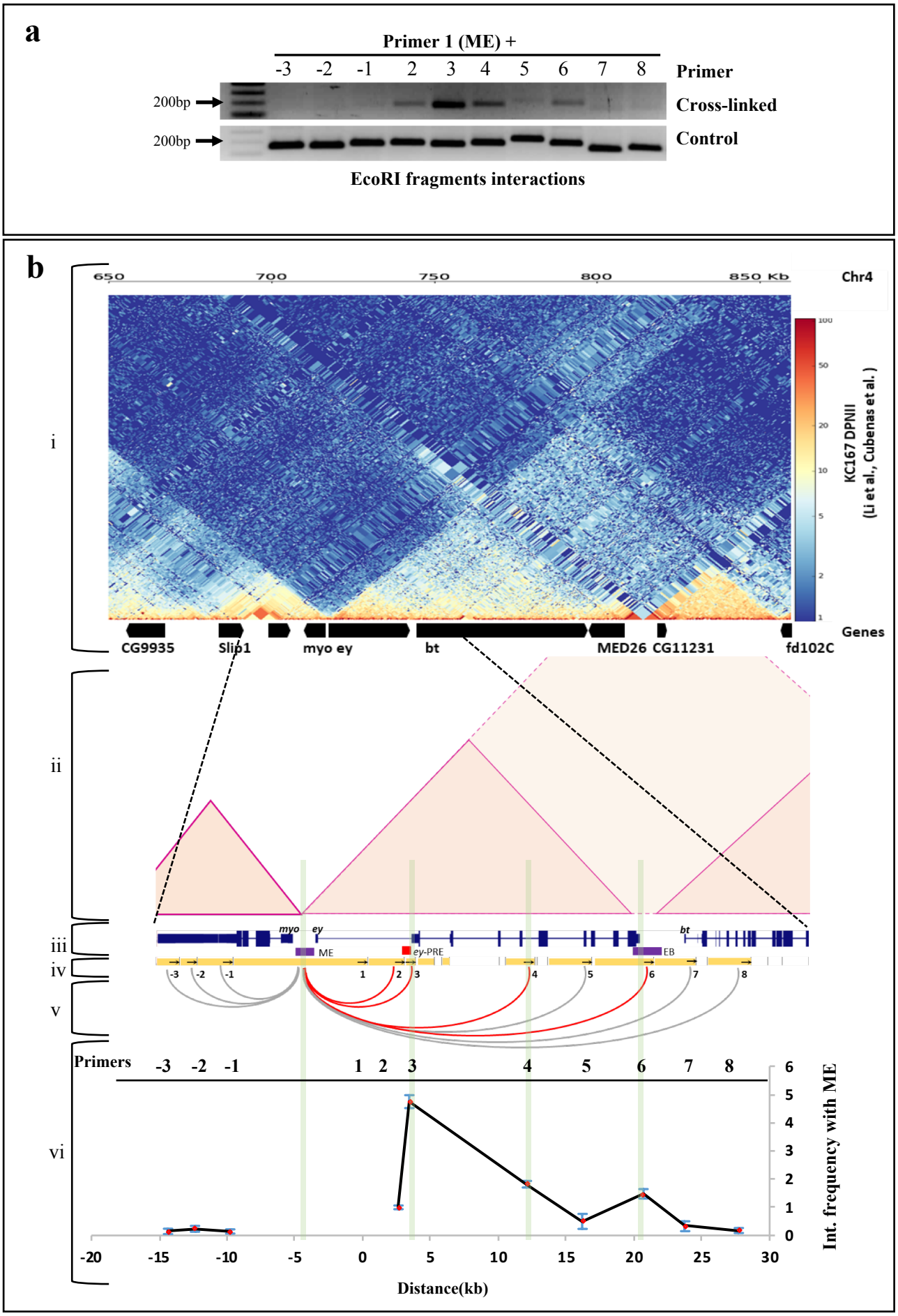
a
Primer 1 (ME) +
-3 -2 -1 2 3 4 5 6 7 8
Primer
200bp
Cross-linked
200bp
Control
EcoRI fragments interactions
b
650 700 750 800 850 Kb
Chr4
i
KC167 DPNII
(Li et al., Cubenas et al.)
Genes
CG9935
Slip1
myo ey
bt
MED26 CG11231
fd102C
ii
iii
iv
v
myo
ey
bt
ME
ey-PRE
EB
-3 -2 -1 1 2 3 4 5 6 7 8
Primers
vi
Int. frequency with ME
Distance(kb)

Figure 7

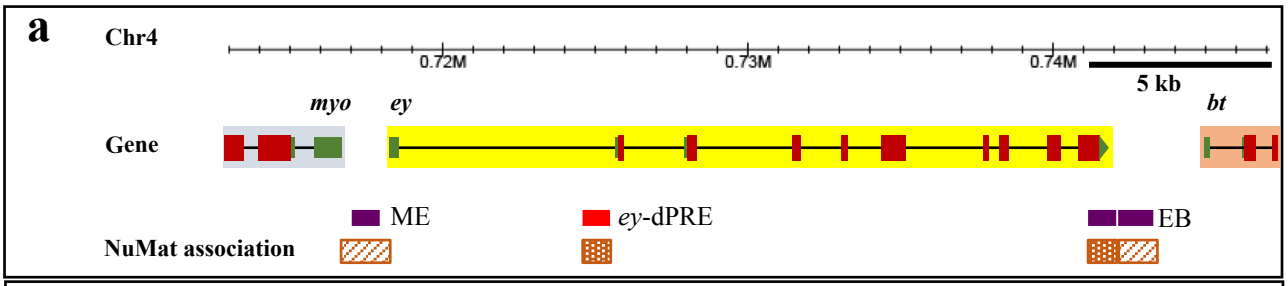
a
Chr4
0.72M
0.73M
0.74M
5 kb
myo
ey
bt
Gene
ME
ey-dPRE
EB
NuMat association

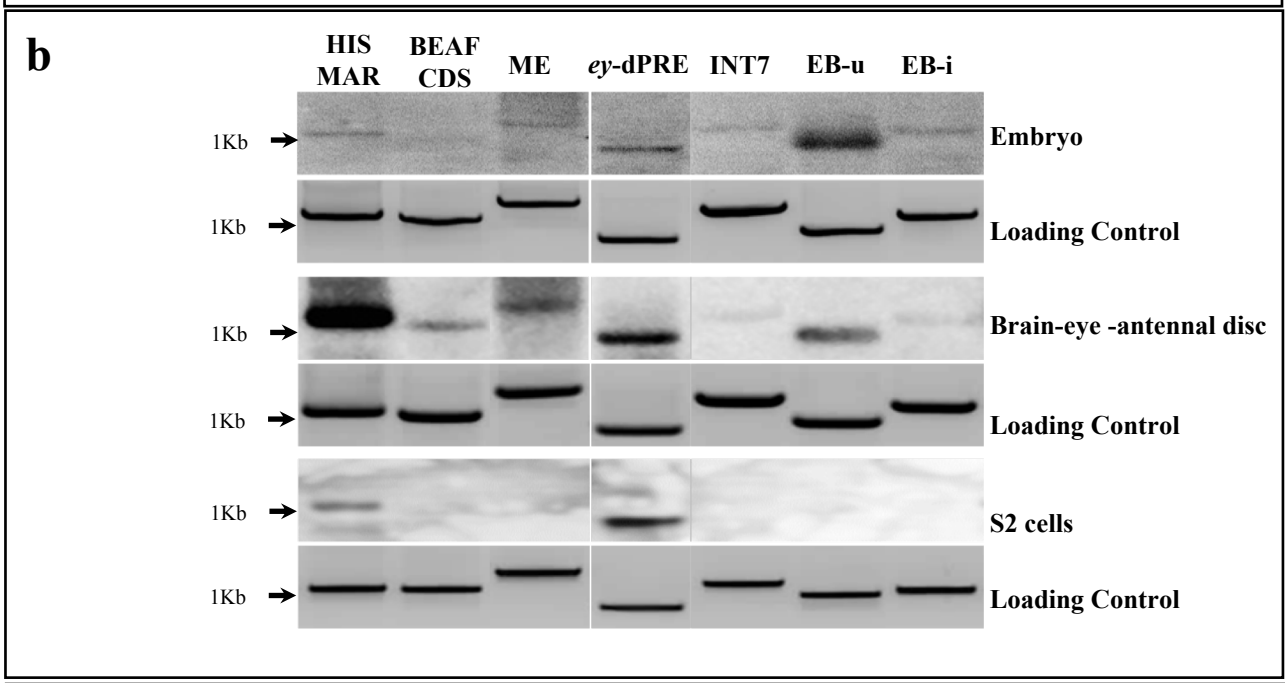
b
HIS MAR
BEAF CDS
ME
ey-dPRE
INT7
EB-u
EB-i
1Kb
Embryo
Loading Control
Brain-eye -antennal disc
Loading Control
S2 cells
Loading Control

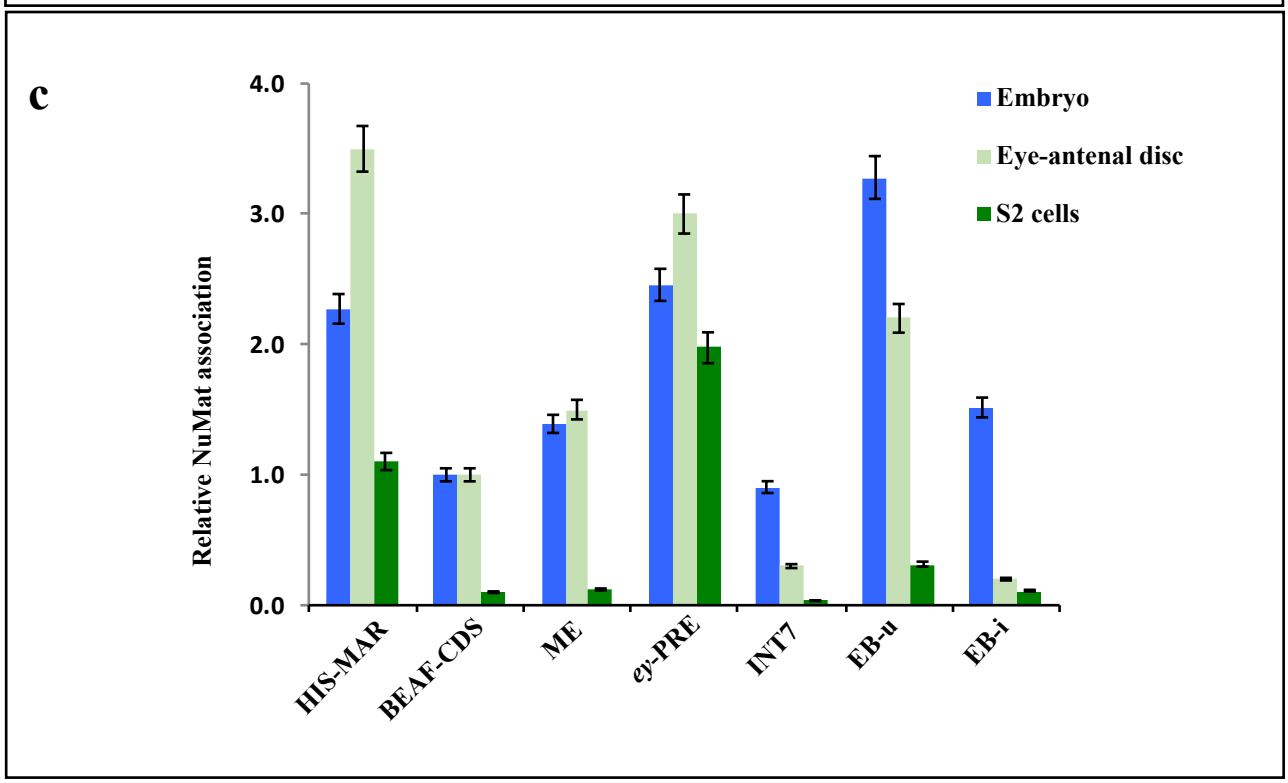
c
Relative NuMat association
4.0
3.0
2.0
1.0
0.0
Embryo
Eye-antenal disc
S2 cells
HIS-MAR
BEAF-CDS
ME
ey-PRE
INT7
EB-u
EB-i

Figure 8

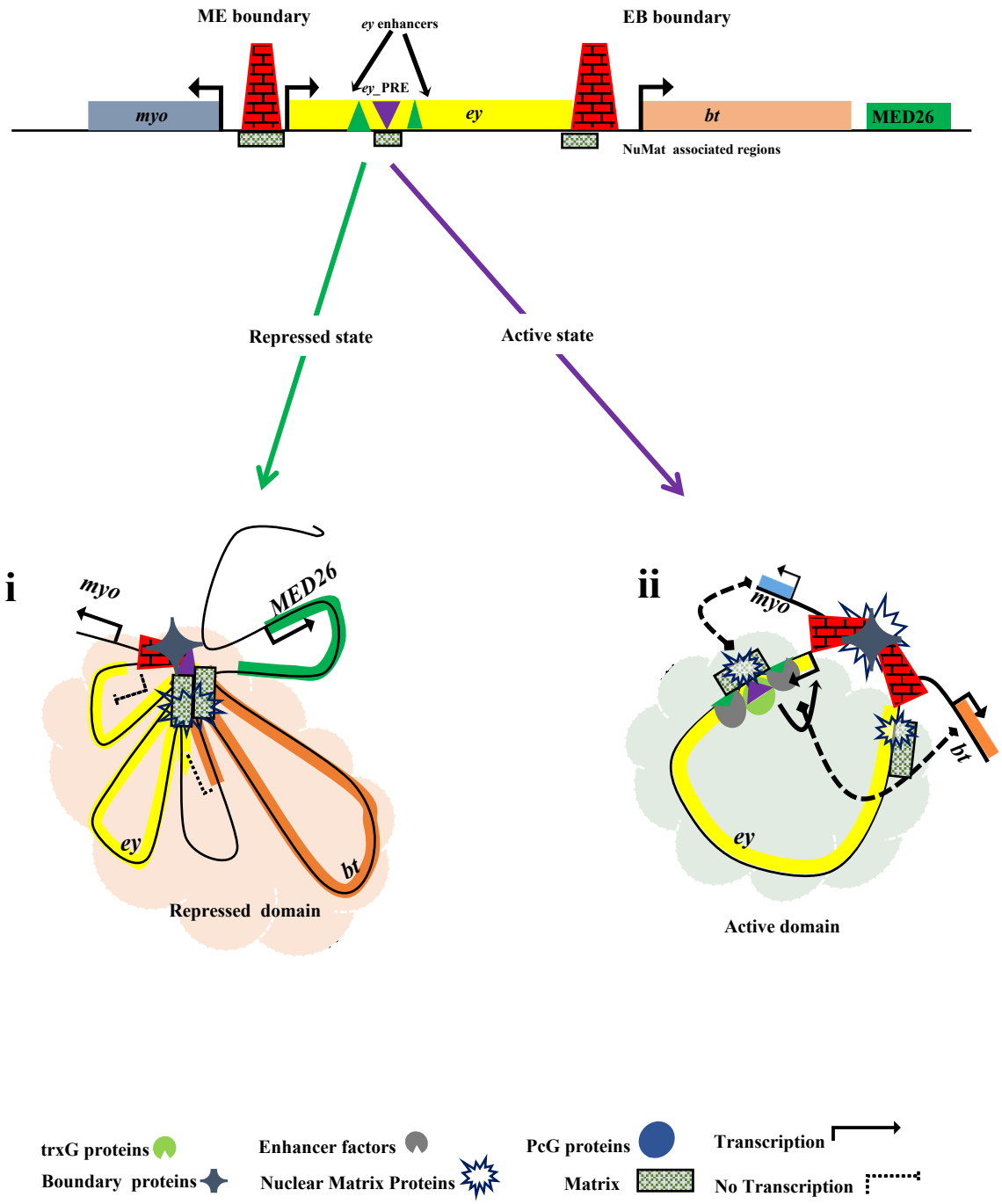
ME boundary
ey enhancers
EB boundary
ey_PRE
myo
ey
bt
MED26
NuMat associated regions
Repressed state
Active state
i
myo
MED26
ey
bt
Repressed domain
ii
myo
bt
ey
Active domain
trxG proteins
Boundary proteins
Enhancer factors
Nuclear Matrix Proteins
PcG proteins
Matrix
Transcription
No Transcription